DEVAN JESSIE AARON RUDOLPH

DESIGN OF A TILT-WING UAV TO INVESTIGATE AND VALIDATE STABILITY IN PITCH AND ROLL

2023

UNIVERSITY OF KYRENIA

INSTITUTE OF GRADUATE STUDIES

AVIATION SCIENCES – AERONAUTICAL ENGINEERING

DESIGN OF AN ELECTRICALLY POWERED DUAL MOTOR TILT-WING UAV TO INVESTIGATE AND DEVELOP AN AUTOMATED STABILITY SYSTEM FOR PITCH AND ROLL CONTROL IN TAKEOFF, HOVER AND LANDING FLIGHT MODES

DEVAN JESSIE AARON RUDOLPH

K20210832

SUBMITTED TO THE INSTITUTE OF GRADUATE STUDIES
IN PARTIAL FULFILLMENT OF THE REQUIREMENTS OF THE DEGREE OF
MASTER OF SCIENCE IN AVIATON SCIENCES - AERONAUTICAL ENGINEERING

Kyrenia

June, 2023

UNIVERSITY OF KYRENIA

INSTITUTE OF GRADUATE STUDIES

AVIATION SCIENCES – AERONAUTICAL ENGINEERING

DESIGN OF AN ELECTRICALLY POWERED DUAL MOTOR TILT-WING UAV TO INVESTIGATE AND DEVELOP AN AUTOMATED STABILITY SYSTEM FOR PITCH AND ROLL CONTROL IN TAKEOFF, HOVER AND LANDING FLIGHT MODES

MSc Thesis

DEVAN JESSIE AARON RUDOLPH

Supervisor

Prof. Dr. Suleyman Tolun

Kyrenia

June, 2023

DECLARATION

I hereby declare that this is my original work and has never been presented for a degree or any award in any university or any academic institution of higher learning. It is all the result of my own effort and under the supervision of ..Prof. Dr. Suleyman Tolun..

Student

..Devan Rudolph..

Signature..

Date ..07../..06../..2023..

Supervisor

..Prof. Dr Suleyman Tolun..

Signature..

Date ..07../..06../..2023..

APPROVAL

The jury members certify that the study conforms to acceptable standards of scholarly presentation and is fully adequate in scope and quality as a dissertation for the degree of Master of science in Aviation Sciences - Aeronautical Engineering.

University of Kyrenia

Academic year: 2022-2023

For jury committee:

Prof. Dr. Süleyman TOLUN _____

..... _____

..... _____

Institute of Graduate Studies Director:

Prof. Dr. Candan ÖZOĞUL _____

Acknowledgments

I would like to express my deepest gratitude to my advisor, Prof. Dr. Suleyman Tolun and also Asst. Prof. Dr Mohsen Soori for their invaluable guidance, support and encouragement throughout the course of my graduate studies. Their expertise and knowledge have been instrumental in the successful completion of this thesis.

I would also like to extend my appreciation to my mentor and close friend, Dr. Pavel Makarov, for his invaluable support and encouragement throughout the research process. His knowledge and expertise have been an inspiration to me.

I am also grateful to my colleague and close friend Ahmed Zakwan for his support, encouragement, helpful suggestions and ideas.

My family has been a constant source of love and support throughout my life and academic journey. I am deeply grateful to them for their unwavering support and encouragement.

Lastly, I would like to extend my gratitude to all my colleagues at Near East University Robotics Laboratory for their support and assistance throughout the research process.

Devan Jessie Aaron Rudolph

Abstract

DESIGN OF AN ELECTRICALLY POWERED DUAL MOTOR TILT-WING UAV TO INVESTIGATE AND DEVELOP AN AUTOMATED STABILITY SYSTEM FOR PITCH AND ROLL CONTROL IN TAKEOFF, HOVER AND LANDING FLIGHT MODES

Devan Jessie Aaron Rudolph
MSc, Aviation Sciences - Aeronautical Engineering
June 2023, 82 pages

Unmanned Aerial Vehicles (UAVs) are defined as aircraft which are operated without the presence of an onboard human pilot. UAVs have found a market niche wherein which they can fill, for as long as their flight performance, automated stability and control and their endurance can be optimized. They can be made use of in multiple environments where human presence might be deemed unsafe or the task at hand might be time consuming or more expensive, on a human level. Such operations may include use in the military, search and rescue missions, intelligence gathering, geo-photography and payload delivery. Following such trends, the development of a tilt-wing UAV has been sought to meet such requirements, more specifically, with applications in heavy payload delivery. It is to this end that an Electrically Powered Tilt-wing UAV has been developed using resources from Near East University, Robotics Laboratory. The models developed as per the required performance illustrated that a more high-fidelity set of mathematical models was required to satisfy the tilt-wing stability requirements in hovering flight mode. It is to this end that a series of test benches were designed and built in order to test and validate the mathematical models before being directly implemented on the UAV in an open-world environment. The control algorithm used for automated stability of the UAV is a PID controller, which has become an industry standard. The governing equations for the P and PD-controller have been analytically derived; and finally, a comparison is made between the analytical model and real world experimental results. This is done in order to validate the model and demonstrate how robust it is.

Keywords: Vertical Takeoff and Landing, Unmanned Aerial Vehicle, PID Controller, Tilt-Wing

Summary

The design of an electrically powered dual motor tilt-wing UAV aims to explore and advance the development of an automated stability system for pitch and roll control during takeoff, hover, and landing flight modes. This innovative unmanned aerial vehicle (UAV) incorporates two motors and a tilt-wing mechanism to enhance maneuverability and adaptability in various flight scenarios. By integrating an electric power system, the UAV offers a sustainable and efficient alternative to traditional fuel-based propulsion.

The primary objective of this design is to investigate and refine an automated stability system that ensures precise control over pitch and roll during critical flight phases. Takeoff, hover, and landing are inherently challenging flight modes that require careful management of stability and control to guarantee safe and controlled operations.

With its dual motor configuration and tilt-wing mechanism, the UAV can transition between vertical takeoff and landing (VTOL) and fixed-wing flight modes, providing increased versatility for different mission requirements. The electric propulsion system not only reduces environmental impact but also offers improved power efficiency and quieter operation compared to conventional engines.

By focusing on the design of an electrically powered dual motor tilt-wing UAV and incorporating an automated stability system, this project aims to contribute to the advancement of UAV technology. The research and development conducted within this framework have the potential to enhance the safety, reliability, and performance of UAVs in critical flight phases, further expanding their applications in various fields, including aerial surveillance, cargo delivery, and environmental monitoring.

Keywords: Vertical Takeoff and Landing, Unmanned Aerial Vehicle, PID Controller, Tilt-Wing

Table of Contents

List of Tables

List of Figures

List of Abbreviations

VTOL: Vertical Takeoff and Landing

UAV: Unmanned Aerial Vehicle

PID: Proportional Integral Derivative

MTOW: Maximum Take-off Weight

PLA: Polyactic Acid

PCB: Printed Circuit Board

IMU: Inertial Management Unit

List of Symbols

K_p : is a term for the p-coefficient containing the expression $\frac{Fhk_p}{J}$

K_i : is a term for the i-coefficient containing the expression $\frac{Fhk_i}{J}$

K_d : is a term for the d-coefficient containing the expression $\frac{Fhk_d}{J}$

k_p : Denotes the 'P' component, which is the changeable parameter in the model

k_i : Denotes the 'I' component, which is the changeable parameter in the model

k_d : Denotes the 'D' component, which is the changeable parameter in the model

M_{lat}: Moment about the aircraft lateral axis: y-axis

M_{long}: Moment with respect to the aircraft longitudinal axis: x-axis

F: Force (Thrust from motor(s))

h: Moment arm

$\ddot{\theta}$: Pitch angular acceleration of the UAV

J_y Moment of Inertia with respect to the lateral axis: y - axis

θ: Pitch angle

φ: Tilt-wing angle (angle at which the tilt-wing is set. In hover this angle starts at 90 degrees with respect to the UAV's longitudinal axis, which is an imaginary line that runs from the nose to the tail.)

m: A constant which determines the rate at which the exponential function decays or grows

τ: Latency (time-delay in transmission, reception and implementation of the commands carried by the signal from the ground control station to the UAV)

CHAPTER I

Introduction

Current trends in the aviation industry are such that they are aimed in the direction of electrifying aircraft. Such ambitious efforts are becoming more and more commonplace as the world tends to move towards more environmentally friendly emission-free propulsion systems. The aim to achieve such systems lies in the desire to preserve the environment by reducing aviation's current global carbon footprint. Beyond the environmental concerns lies the subject of taking advantage of renewable energy sources such as rechargeable power sources for the electrification of aircraft. The benefits which can be realized from implementing such advanced technological solutions will be evident in cost savings as operators of such aircraft will not need to pay for the comparably more expensive conventional jet fuel and this will translate to much cheaper tickets for passengers using the services of such aircraft (if they are passenger aircraft) and generally lower operating costs. The other benefits which can be immediately realized from the electrification of aircraft is that of lower maintenance cycles per flight hour (or nautical mile). Given that electric aircraft generally have fewer components with respect to the propulsive system and also an absence of the complex web of fuel lines, fuel management systems, and all related devices found onboard such aircraft, this results in a comparably cheaper aircraft to operate and maintain. It is to this end that the tilt-wing UAV concept presented below has been developed.

This study demonstrates the current activities related to the development of a tilt-wing UAV as a Master Thesis and highlights its application potential based on both current and future market needs. This thesis also surveys current trends in VTOL UAV design and development as far as is necessary for the current project at hand. Particular attention is paid to VTOL UAVs as these configurations bear resemblance in capabilities, but not in performance, to the UAV under development. In order to provide more perspective, a description of the ''differentiating factor'' of the UAV under development is also given.

Research Problem

Over the years, a significant amount of effort has gone into research and development of vertical takeoff and landing (VTOL) UAVs. The main focus of such efforts has been on multi-rotor UAVs, however recently that focus has shifted to tilt-wing and tilt-rotor configurations. In the field of VTOL UAV development, the primary focus has been on UAVs with VTOL capabilities which are made possible by incorporating vertical thrust-providing motors for take-off and landing, in addition to either a pusher or tractor type of motor configurations to facilitate forward flight. Such motor configurations and placements have become quite common as they are a simple solution to providing stability for the UAV in both VTOL and transition flight modes.

The world has begun to embrace the possibilities that can be realized by leveraging UAV technologies in urban air mobility, search and rescue missions, cargo transportation and delivery, and intelligence gathering. Several aircraft manufacturers have developed and tested UAVs, most of which are still currently at the experimental stages. Several configurations have been tested over the years, however, very little attention has been given to dual motor VTOL UAVs, and this is primarily because the stability requirements for either a tilt-wing or tilt-rotor UAV are such that a seemingly complex automated stability system is required to keep the UAV stable in both VTOL and hover modes. Most current research and development work focuses on VTOL UAVs which have three to four motors for flight stabilization. This is done because it is much easier to stabilize and control such an aircraft.

As seen in both literature and practice, the guidance, stability and control of VTOL UAVs can be achieved in several ways. The methods used depend on the kind of aircraft in question and its intended mission. The tilt-wing UAV developed and presented in this work has demonstrated a good response in roll and pitch control in hover mode. Such an achievement is important in order to ensure a good and predictable response of the UAV to any disturbances during its flight operations. Roll and Pitch stability have been verified and validated on a scaled-down prototype mounted on a test-bench and such potential disturbances as may be seen in real world applications affecting roll and pitch control are manually simulated.

Significance of the Study

The advantages that come with the implementation of UAVs are significant. From their high level of autonomy to their ease of operations in terms of a lesser amount of man-power required to operate them, the scope and scale of their benefits is left to one's imagination

This study aims to develop an Electrically Powered Tilt-Wing UAV that serves as a platform to demonstrate the fine-tuned and optimized stability and control capabilities of a dual motor tilt-wing UAV in hover mode. A refinement of the results obtained in the study are expected to be able to be used in such future iterations of the given aircraft configuration.

Limitations

The subject under study has a very limited amount of historical information from which a foundation can be laid. As such, most investigations into the subject and most techniques used had to be developed based on a very limited amount of information, leading to the development of unique solutions. This increases the level of complexity of the research and development work.

Motivation

The global economy has begun to appreciate the true potential of the implementation of UAV technologies. It is not a stretch of the imagination to understand the numerous benefits that come with the use of UAV services. Search and rescue missions can be made more efficient in terms of area covered in a specific amount of time during a search; intelligence gathering and surveillance missions can be executed without the additional costs of an on-board human pilot, and depending on the level of autonomy of the UAV, without the need of large number of ground operations personnel; delivery missions can be carried out in a significantly shorter amount of time at a competitive price point; urban air mobility can become a reality as VTOL UAVs become safer and more common place; UAVs can be used in wildlife tracking and anti-poaching; UAVs can also be used in agriculture in spraying pesticides on crops and also monitoring soil quality.

Their operations can also be implemented in geo-photography, and mapping. Such use cases have significantly spurred the development and advancements of these aircraft.

Problem Statement

The challenges seen in the aviation industry with respect to tilt-wing/tilt-rotor VTOL UAV developments are compounded by little to no exhaustive literature on the subject. The development of the Bell Boeing V-22 Osprey is one of the more exceptional cases for the large scale practical implementation of tilt-rotor technology. However, even during its initial development, the Osprey was riddled with control issues which led to a series of failures during operations

The main objective of this work is to mathematically model, develop and test an automated stability system for an electrically powered tilt-wing VTOL UAV in hover mode. The automated stability system is designed in such a way as to ensure a safe and effective response of the UAV to any disturbances during hover flight modes. Such a solution has been attempted due to an observed industrial need for such technical approaches. It is to this end that a scaled down tilt-wing UAV prototype was designed and manufactured using 3D-printing technology and used as a ‘’test-bench’’ platform for the initial implementation of the system. The design was inspired by the hover capabilities of conventional helicopters and also the forward flight speed, range, endurance and maneuverability of fixed wing aircraft. It is generally known and accepted that fixed wing aircraft offer more efficient cruise performance over a long range whilst helicopters offer better hover performance, greatly exceeding that of common multi-copters. It is to this end that the development of a tilt-wing UAV was conceived of for this particular purpose.

The thesis also develops a MATLAB model for selecting PID coefficients thus reducing the cumbersome tasks of conventional PID tuning leading to a more refined narrow field of PID values from which initial coefficients can be selected.

Thesis Layout

In chapter 1, An introduction into unmanned aerial vehicles, project definition, significance of the study, limitations and motivation for the project.

In chapter 2, A more detailed discussion of unmanned aerial vehicles is presented, together with a deep dive in types of control systems and what is available in the market. A discussion on which is the most preferred method for this thesis is also mentioned.

In chapter 3, An analytical approach to the project is looked at, which forms a base for the experimental stage of the project.

In chapter 4, The methodology used in the experiment, electronic components and the setup of the experiment done in the project are all mentioned in this chapter.

In chapter 5, Results from the experiment are compared to the analytics done in this chapter together with their discussion.

In chapter 6, A conclusion and future scope for further research is discussed in this chapter.

CHAPTER II

Literature Review

About two decades ago, the idea of unmanned aircraft technologies was still in the early stages of its development (Guillaum et al, 2021). Not much work had been done and there was little to no literature and test data available for ambitious designers to look to. Over the years, there has been a significant amount of technological development and advancements in the field of unmanned aerial vehicles. As the scope of their applications has increased, academic and industrial interest in their applications has also increased. With such a positive outlook for the possibilities in their applications, investment in UAV development has significantly increased in both government and private sectors. This has led to the establishment of companies and related research and development facilities specializing in the design and development of unmanned aerial vehicles. These companies and organizations have come to realize that the applications of these UAVs are of significant importance in both humanitarian and profitable ways.

Major aerospace manufacturers such as Bell Helicopters and Boeing have been successful in developing and deploying the Bell-Boeing V22 Osprey; a tilt-rotor aircraft used used by the United States Marine Corps. Such an aircraft has been instrumental in assisting ground troops in its major areas of application and also in transportation of both payloads and troops. Aircraft with VTOL capabilities such as the V22 Osprey are streamlining operations within the military as we know it. However, as per this current work, such capabilities should also be made available for civilian use. It is to this end that companies such as Lilium Jet, Auto Flight, Dufour, Arcturus UAV, L3 Harris Technologies and Autel Robotics have developed VTOL UAVs capable of executing the intended missions for which they were designed.

Given that there are several classes of VTOL UAVs, it is here that a brief description of each will be given.

1. *Tail-Sitter Aircraft*

As implied by the name, tail-sitter aircraft takeoff and land vertically on their tail. For such aircraft, the motors are rigidly attached to the air frame and so it is the entire aircraft that rotates to achieve forward flight. The transition to and from forward flight modes is achieved by aerodynamically manipulating the control surfaces or thrust vectoring of the motors (Guillaum et al, 2021). Tail-sitters are typically more mechanically simple as they do not generally require complex rotating mechanisms to facilitate any transitions between flight modes and as such, these aircraft are typically lighter. One of the major drawbacks of such aircraft is their large exposed surface area which when exposed to wind makes them less maneuverable and very difficult to control during VTOL operations. This greatly reduces the hover efficiency of the tail-sitter aircraft as more energy is required to stabilize the aircraft. Another major draw back of tail-sitter aircraft is that they experience a higher angle of attack during low speed operations which can easily lead to a stall.

2. *Tilt-Wing UAV*

As the name suggests, for the case of tilt-wing aircraft, the motors are rigidly attached to the wings in such a way as to ensure that the wings and motors rotate together as a single collective unit. During such a rotation, the fuselage can be assumed to remain relatively horizontal with small changes in pitch angle (Guillaum et al, 2021). The ability to tilt is facilitated by the implementation of additional tilting actuators which tend to increase the mechanical complexity of such aircraft and this may lead to actuation delays in the system. Similar to tail sitters, the exposed large surface area of the wing increases sensitivity of the wing to wind gusts during takeoff and landing (Jeffrey J. Dickeson et al, 2007). With regards to cruise efficiency, the fixed position of the propellers with respect to the wing allows for the aerodynamic optimization of the wing in order to improve its aerodynamic efficiency and performance in forward flight.

Since the motors are fixed to the wing of the aircraft, this allows for various design options for the wing geometry and therefore leads to significant enhancements of the aerodynamic efficiency and performance of the aircraft.

Due to the requirement for the presence of a wing-tilting mechanism, conventional aircraft configurations are technically the most suitable . For the case of tilt-wing aircraft implementing the quad tilt-wing, all four rotors tilt, sometimes located on two sets of wings. Such configurations are not the most optimal as the need arises for the presence of two sets of tilting mechanisms, one four each wing, the front and the rear; this tends to increase both the weight and complexity of the design.

3. *Tilt-Rotor UAV*

Like tilt-wing aircraft, tilt-rotors belong to a group of aircraft called convertiplanes. For the case of tilt-rotor aircraft, the motors are attached to the wings in such a way as to facilitate the rotation of the motors independent of the wings. The rotation of the motors is made possible through the implementation of a tilting mechanism which is added to the motors. It is by this method that the thrust vector is rotated vertically for takeoff and landing flights and is rotated horizontally to achieve forward flight (Adnan S. Saeed et al, 2015).

One of the first drawbacks of the tilt-rotor configuration is the presence of a part of the wing being being located in the propeller wash. This has been observed to generally reduce the propeller thrust. A thorough analysis of such aerodynamic interferences and their effects are found in the publication (H. Yeo et al, 2009).

Some tilt-rotors tend to have fixed rotors which are always pointed upwards. This is done in order to simplify the mechanical design of the aircraft and provide VTOL capabilities during takeoff, hover and landing flight modes (Adnan S. Saeed et al, 2015). An example of a production manned tilt-rotor aircraft is the Bell Boeing V22 Osprey. The design of tilt-rotor aircraft is such that they typically feature engines that are mounted at the wing tips. This design solution forces the use of a wing with a reduced span and a much thicker airfoil (Adnan S. Saeed et al, 2015). This may result in increased drag and poor aerodynamic performance. However, it is worth noting that for the case of tilt-rotor aircraft, the tilting mechanism is required to rotate only the motors and not the the wings or any other heavy structures and so savings in power may be achieved.

Current VTOL UAVs Being Tested and Developed in Industry

Table 2.1 Current electric powered VTOL UAVs

Aircraft	Configuration	Number of Wing/Motors	Uses
Dufour	Tilt-Wing UAV	Quad-Motor Monoplane	Payload Transportation
Lilium Jet	Tilt-Rotor	36 electric motors	Urban Air Mobility
Arcturus T-20 Jump VTOL	Fixed wing with seperate motors for VTOL flight and Forward flight	5 electric Motors	Payload Transportation
Vector eVTOL UAV	Multicopter	3 Electric Motors	ReconnaissanceUAV
FVR-90 VTOL UAV: Hybrid	Fixed wing with seperate motors for VTOL flight and Forward	5 electric Motors	Payload Transportaion
Dragon Fish Tilt-Rotor VTOL UAV	Tilt-Rotor	4 Electric Motors	Aerial Photography, Aerial Inspections

The current dominant industrial trends in VTOL UAV development implement VTOL stabilization systems which utilize more than two motors to balance the UAV during vertical flight operations (hover mode). This approach greatly simplifies the stabilization requirements of the UAV in hover mode by simply providing a triangular set-up of motors or a quad-copter-like configuration which ensures stability. In as much as this is a practical solution which works, it is not the most efficient or most optimum solution as it tends to increase the mechanical complexity of the UAV, it increases operating costs in terms of having more motors to power, service and maintain, it degrades the aerodynamics of the UAV in forward flight as the UAV will have more protruding parts interacting with the air flowing over it, and it also adds weight to the UAV which will increase power consumption. Another common UAV design for VTOL flight is the quad-copter. Such a UAV has certain advantages which it offers in terms of hover capabilities,

ease of deployment, quick turn-around time, ease of navigation and operation in confined spaces. The key disadvantages are; they generally fly at slow speeds, higher power consumption, shorter range, and lower payload capabilities when compared to fixed wing aircraft. With these key disadvantages in mind, the most optimum solution is to minimize the number of required motors on board and implement fixed-wing forward flight capabilities.

Fixed wing aircraft are typically faster and more maneuverable than multi-copter aircraft (and even helicopters), and it is to this end that a fixed wing configuration is deemed the most ideal.

This current study was inspired by the hover capabilities of conventional helicopters and also the forward flight speed, range, endurance and maneuverability of fixed wing aircraft. It is generally known and accepted that fixed wing aircraft offer more efficient cruise performance over a long range whilst helicopters offer better hover performance, greatly exceeding that of the common multi-copters. It is to this end that the development of a tilt-wing UAV was conceived of for this particular purpose.

The development of a UAV which satisfies the hover capabilities of a helicopter and also achieves the forward flight speeds, maneuverability and efficiency of fixed-wing aircraft is of great importance as such aircraft are known to be more efficient than current multi-copters.

Fig 2.1 Dragon Fish Tilt-Rotor UAV (Source: https://ired.co.uk/store/autel-dragonfish/)

Fig 2.2 FVR-90 VTOL UAV: Hybrid (Source: https://www.l3harris.com/all-capabilities/fvr-90-airframe)

Fig 2.3 Dufour UAV (Source: https://www.dufour.aero/)

Fig 2.4 Lilium Jet (Source: https://lilium.com/jet)

Fig 2.5 Arcturus T-20 Jump VTOL (Source: https://www.avinc.com/uas/jump-20)

Fig 2.6 Vector eVTOL UAV (Source: https://quantum-systems.com/vector/)

The survey of current VTOL UAV technologies being developed today indicates that there is a need for a more robust automated stabilization system for UAVs in VTOL flight modes if optimum efficiency and controllability are to be achieved. Current industrial solutions make use of multiple motors to balance and stabilize the UAV during VTOL flight, however such techniques lead to an increase in power consumption for the aircraft. This becomes particularly important when considering aircraft which are designed in such a way as to be powered by electric propulsion systems.

For all electric powered aircraft, one of the main areas of prime importance is that of minimizing the weight of the batteries and in that way, also minimizing the power consumption by the aircraft. It is to this end that reducing the weight of the aircraft and reducing the number of power intensive components is of significant importance.

In order to minimize the MTOW of an electric powered tilt-wing UAV, the number of motors can be minimized, ideally using only 2 motors for takeoff, cruising, hovering and landing. However, in order to achieve an controllable and efficient system with a safe response to any disturbances during hover, takeoff and landing, a robust automated stability system has to be developed and implemented.

The two main disturbances of prime importance with respect to the operational safety and response of a tilt-wing UAV during hover are disturbances which effectively cause changes in roll and pitch attitudes of the UAV. It is generally understood from practice that attempting to manually stabilize a tilt-wing/tilt-rotor aircraft of any sort is close to impossible as human beings have a very limited reaction time to effectively correct any undesirable changes in attitude.

The automated stability and control of convertiplanes is still a great challenge today (Guillaum et al, 2021). There are several control systems that have been developed and implemented in Industry. It is to this end that a PID controller has been developed and implemented in the tilt-wing UAV under study.

Definition of The Axis System Used

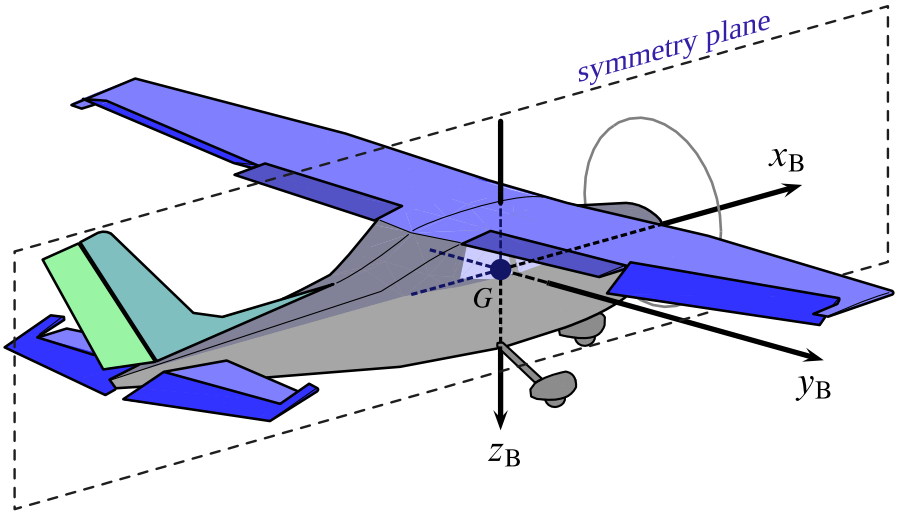

Fig 2.7 Axis System Used (Source: https://jsbsim-team.github.io/jsbsim-reference-manual/mypages/user-manual-frames-of-reference/)

References to moments, torques and accelerations are made with respect to the body axis of the UAV

CHAPTER III

Theory and Modeling

Proper modeling is of great importance for any form of simulation and control of convertible aircraft. Convertible aircraft such as tilt-wing and tilt-rotor aircraft generally combine two fundamental features:

1. an actuation system that is capable of facilitating the transition to different flight modes

2. an air frame that has some wing(s) capable of producing the necessary lift at some sufficient forward flight speeds.

The automated stability and control of convertible UAVs is still a great challenge today. This comes about as a result of highly non-linear dynamics which tend to result from different aerodynamic effects. The transition maneuvers which are executed between helicopter and fixed wing modes and vice versa are naturally very complex as the flight control system is typically required to handle very large changes in the wing angle of attack (AoA), particularly for convertible aircraft such as tail-sitters and tilt-wing aircraft. The large changes in angle of attack, velocity, attitude and actuator effectiveness have strong effects on the aerodynamic forces and moments/torques which are seen to act on the vehicle.

One of the major difficulties that come from the more classical methods of capturing these dynamics characteristics, such as making use of computational fluid dynamics tools or wind tunnel analysis is that these methods do not provide analytical expressions which capture the dynamics of the system. With respect to designing a control system capable of stabilizing the aircraft, these methods become more useful when one needs to finely tune a controller around a given flight velocity (Guillaum et al, 2021). It is with this knowledge that a PID controller was designed and implemented to stabilize the UAV in VTOL flight. At this stage, transition to forward flight is not considered.

UAV Under Development (Named LANNER)

The UAV under study has been developed as a dual motor electrically powered tilt-wing UAV which takes advantage of the hover capabilities and efficiency of a helicopter and the forward flight speeds, range, cruise, high endurance, high maneuverability and payload capacity of fixed wing aircraft. Lanner sees potential applications in payload delivery and can be retrofitted to execute search and rescue missions.

Table 3.1 Main features and advantages of the ongoing design

MAIN FEATURES	ADVANTAGES
Single Tiltwing	Weight Efficiency, Structural efficiency and simplicity.
Two motors	Weight efficiency, Lower power consumption
Yaw control by the aileron in Hover mode	Improved maneuverability, Simplified control system, efficient use of control surfaces
Thrust differential for yaw control in forward flight	Weight efficiency, Simplified design

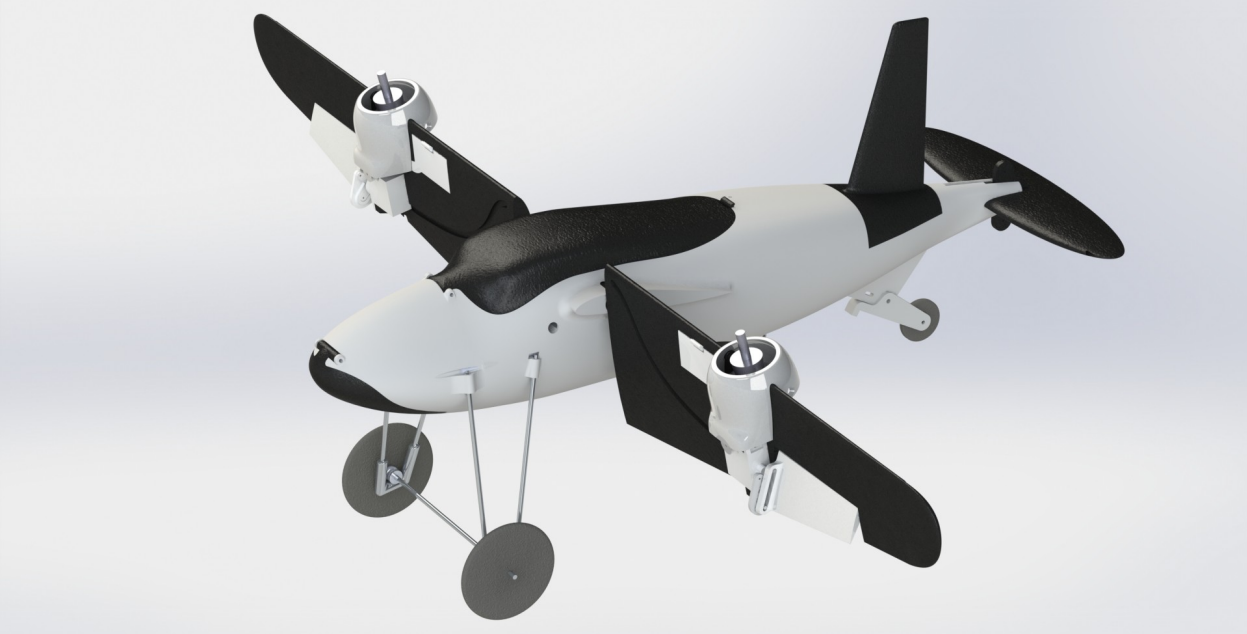

Fig 3.1 Lanner Rendered in VTOL Mode

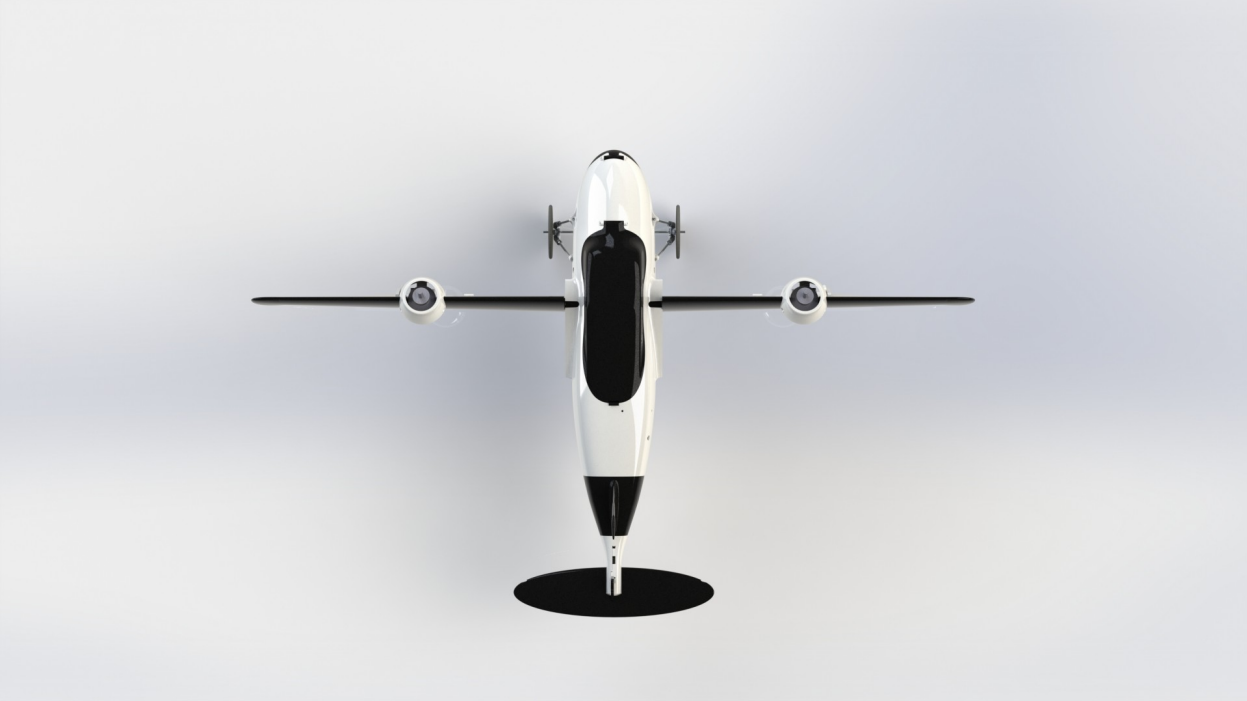

Fig 3.2 Lanner's Top View Render

The mechanical design of the UAV is such that it takes advantage of the thrust line of the motors being placed in line with the center of gravity. This allows the UAV to be balanced during takeoff and hover, and also during landing.

Given that the UAV is balanced by virtue of the thrust line cutting through the center of gravity, it stands as being ''mechanically stable''. However, in the event of a disturbance interacting with the UAV, a stabilization system has to be developed and implemented.

Since Lanner is a tilt-wing aircraft that is solely powered by two electric motors, each located on either wing, it requires a robust automated stabilization system to counteract any disturbances and also make necessary corrections of any unwanted changes in attitude in both roll and pitch during hover. Lanner has been developed with this two-motor configuration in order to satisfy an existing market niche which demands such capabilities.

The two main disturbances of prime importance with respect to the operational safety and response of the UAV are disturbances which effectively cause changes in roll and pitch attitudes of the UAV. It is generally understood from practice that attempting to manually stabilize a tilt-

wing/tilt-rotor aircraft of any sort is close to impossible as human beings have a very limited response time to effectively correct any undesirable changes in attitude. It is to this end that a PID controller was developed and implemented.

The PID controller makes corrections to any undesirable changes in roll and pitch during hover. It is this PID controller that stabilizes the UAV.

Standard PID Controller Algorithm Implemented:

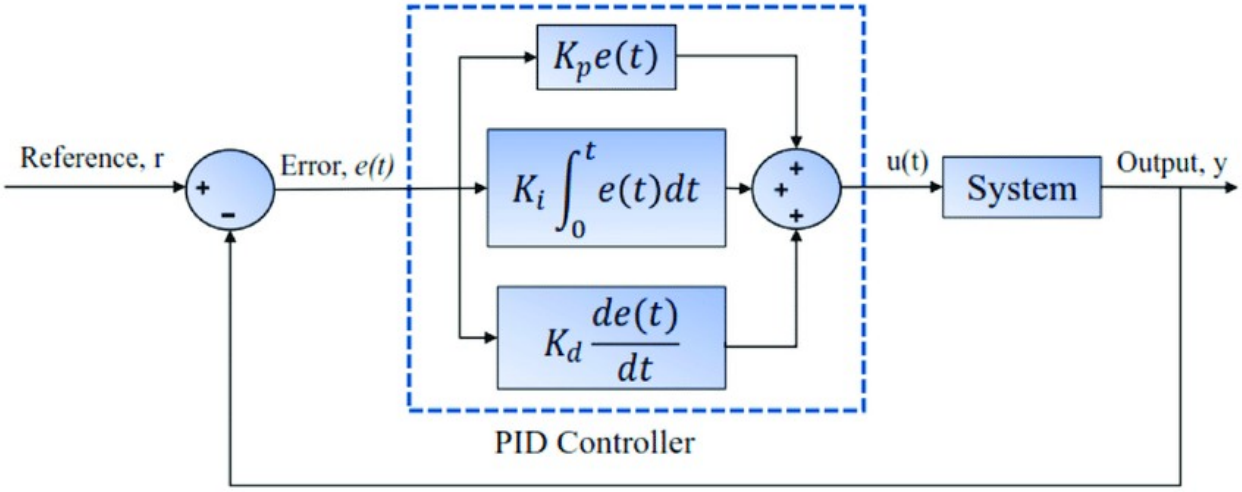

Fig 3.3 Block Diagram of a Process Control Using a PID Controller

Controllers generally take the error signal and convert it into a command which is to be executed. PID controllers typically use the past error, present error and a prediction of the future error in such a way that it calculates appropriate actuator commands which will produce the desired output.

The PID controller algorithm is represented by the equation given below:

$$u(t) = K_p e(t) + K_i \int_0^t e(\tau)\, d\tau + K_d \frac{d}{dt} e(t) \tag{3.1}$$

where u is the control signal that is applied to the system

K_p is a term for the p-coefficient containing the expression $\frac{Fhk_p}{J}$,

K_i is a term for the i-coefficient containing the expression $\frac{Fhk_i}{J}$

K_d is a term for the d-coefficient containing the expression $\frac{Fhk_d}{J}$

The PID controller works in such a way as to ensure that the system under control returns to a state of stability by mitigating the oscillations brought about by a disturbance. It is generally made up of three key components which are responsible for stabilizing the system. P, I and D components. Because every process responds differently, the PID controller determines how much and how quickly the correction is applied by using varying amounts of Proportional, Integral and Derivative action. Each component contributes a unique signal that is added together to create a controller output signal. The PID controller is responsible for ensuring that the process remains as close to the desired value as possible regardless of disruptions.

The ‘P’ component, which is the Proportional component, works by correcting some target which is proportional to a difference. The P-controller parameter helps the system approach the target value, however, most of the time, this target value is not achieved simply because as the difference approaches zero, so does the applied correction to the system.

The ‘I’ component, which is the Integral component, creates an output proportional to the duration and magnitude of the error signal. The longer the error, and the greater the amount, the larger the integral output. For as long as an error exists, the integral action will continue.

The ‘D’ component, which is the derivative component, minimizes the overshoot by slowing down the correction factor as the target value is being approached. This helps ensure that the system returns to a state of stability in the event of interacting with a disturbance that may destabilize it.

PID controllers have become a popular option when it comes to implementing system control as they are simple to understand and implement, efficient, stable and robust.

Mathematical Modeling of The Roll Dynamics

Determining the roll dynamics of the UAV is of critical importance during the design process as this enables the system to be designed in such a way as to ensure that it meets and satisfies all safety and control requirements.

In order to develop a rigorous understanding of the UAV roll dynamics, a mathematical model which describes the UAV roll dynamics was developed. The model simulated the roll response to any changes in the attitude of the UAV by effectively binding the roll dynamics to the PID controller.

Knowing this, a solution for the roll dynamics can be achieved in the following way:

From Newton's second law's rotational equivalent, we know that the sum of all moments acting on a system is equal to the product of the system's moment of inertia multiplied by angular acceleration.

The moment created by the motor on the wing will be equal to; (roll model developed from Fig 4.11)

$$M_{long} = Fh \tag{3.2}$$

where M_{Long} is the moment with respect to the longitudinal axis: x-axis,

F is the force from the motors,

h is the length of moment arm

For the case of small changes in the tilt-wing angle, φ,

$$M_{long} = Fh\sin\varphi \tag{3.3}$$

where φ is the tilt-wing angle, which is the angle at which the tilt-wing is set. In hover this angle starts at 90 degrees with respect to the UAV's longitudinal axis, which is an imaginary line that runs along the length of the fuselage, from the nose to the tail: x-axis).

If we assume that φ is a really small angle then,

$$\sin\varphi = \varphi \tag{3.4}$$

Therefore,

$$M_{long} = Fh\varphi \tag{3.5}$$

$$M_{lat} = J_y \ddot{\theta} \tag{3.6}$$

where M_{lat} is the moment with respect to the lateral axis: y-axis,

J_y is the body's moment of inertia with respect to the lateral axis: y-axis.

$\ddot{\theta}$ is the body's pitch angular acceleration with respect to the lateral axis: y-axis.

In order for a relationship between φ and Newton's 2nd law for rotational motion to be determined, we equate the moments as expressed in equations (3.2) and (3.3) ;

$$J_y \ddot{\theta} = Fr\varphi \tag{3.4}$$

$$\varphi = \frac{J_y \ddot{\theta}}{Fh} \tag{3.5}$$

Knowing that the general equation of a PID controller is as given below:

$$u(t) = K_p e(t) + K_i \int_0^t e(\tau)\,d\tau + K_d \frac{d}{dt} e(t) \tag{3.6}$$

For the case under study, the equation will then be written in following way:

$$\varphi(t) = K_p \theta(t) + K_i \int_0^t \theta(\tau)\,d\tau + K \frac{d}{dt} \theta(t) \tag{3.7}$$

θ in the PID expression above is the pitch angle of the UAV, which is the controlled parameter, whereas φ is the tilt-wing angle and as such is effectively the controlling parameter.

It will be highlighted here that during hover mode, the wing is set at an angle of 90 degrees with respect to the longitudinal axis of the fuselage. However, given that this 90 degree angle is the required orientation for the wing in order for it to maintain stable hover, for simplicity, this position is given an initial value of 0 degrees. This way, any changes in the angle due to a disturbance will be taken as a positive or negative increase in this initial angular orientation. It is to this end that when ever a situation arises such that $\varphi = 0$, this would imply that the wing is vertical and there is no torque acting on the UAV system.

Mathematical Modeling of Pitch Dynamics

Pitch Controller Without Latency

In order to develop a rigorous mathematical model of the UAV pitch dynamics, a P controller with no latency was first developed and investigated, then a P controller with latency was developed and investigated.

A P-controller with no latency can generally be described by the following equation below;

$$\varphi = -\left[k_p \theta(t)\right] \tag{3.8}$$

$$\varphi(t) = -\left[k_p \theta(t)\right] \tag{3.9}$$

where φ is the tilt-wing angle,

θ is the pitch angle

k_p is the P-coefficient. This is the changeable parameter in the model

Equations 3.8 and 3.9 are the equations of a P-controller without latency. These equations do not take into account any time delays in transmission of any control signals.

Given that;

$$\varphi = \frac{J_y \ddot{\theta}}{Fh} \tag{3.10}$$

It can then be represented in following way,

$$\frac{J_y \ddot{\theta}}{Fh} = -\left[k_p \theta(t)\right] \tag{3.11}$$

$$\ddot{\theta} = \frac{-Fhk_p}{J_y}\theta(t) \tag{3.12}$$

It is from here that we achieve the differential equation in the following way,

$$\frac{Fhk_p}{J_y} = K_p \tag{3.13}$$

where K_p is a term for the p-coefficient containing the expression $\frac{Fhk_p}{J_y}$

From the relationships given above, we then obtain the second order differential equation given below,

$$\ddot{\theta} + K_p \theta(t) = 0 \tag{3.14}$$

It is this second order differential equation that captures the governing dynamics of the system. The solution to this differential equation then demonstrates the systems response to a disturbance under the influence of a P-controller with no latency. Having no latency is generally an ideal case.

Making the following approximation,

$$\theta = e^{-mt} \tag{3.15}$$

where m is a constant which determines the rate at which the exponential function decays or grows,

t represents the independent variable (such as time) over which the function θ is defined

Then taking the first and second derivative of the equation we obtain the two equations as given below,

$$\dot{\theta} = -m e^{-mt} \tag{3.16}$$

$$\ddot{\theta} = m^2 e^{-mt} \tag{3.17}$$

Making the substitution for $\ddot{\theta}$, we then obtain the equation below, which is in its essence, a quadratic equation and so can be solved as such:

$$m^2 e^{-mt} + K_p e^{-mt} = 0 \tag{3.21}$$

$$m^2 + K_p = 0 \tag{3.22}$$

The solution to the equations will take form given below,

$$m = \pm i K_p \tag{3.23}$$

Given that the general solution of a differential equation contains complex roots, the solution will be in the form given below,

$$\theta(t) = e^{\alpha t} \tag{3.24}$$

Pitch Controller With Latency

There are several factors which may lead to a miss match between theoretical and experimental results. Such factors may include friction which exists between all moving components on-board the system which are difficult to include in the model, component latency in signal transmission and reception, poor motor performance and errors which may arise from assumptions made during the process of mathematical modeling.

This current study models the pitch controller by taking latency into account in order to achieve a result that approximates the experimental results to within an acceptable degree of accuracy.

It is here that a P- controller with latency is developed and a solution modeling the dynamics has been achieved.

The general equation describing a P-controller with latency is as shown below.

$$\ddot{\theta} + K_p \theta(t - \tau) = 0 \tag{3.25}$$

where τ is latency

Solving this differential equation where;

$$\theta = e^{-mt} \tag{3.26}$$

The characteristic equation will then become,

$$m^2 + K_p . e^{-m\tau} = 0 \tag{3.28}$$

Using the following Taylor series approximation,

$$e^{-m\tau} \approx 1 - m\tau + \frac{m^2\tau^2}{2} \tag{3.29}$$

After substituting equation (3.29) into equation (3.28), we then obtain the solution below,

$$m^2 + K_p \left[1 - m\tau + \frac{m^2\tau^2}{2} \right] = 0 \tag{3.30}$$

$$m^2 + K_p - K_p m\tau + \frac{K_p m^2\tau^2}{2} = 0 \tag{3.31}$$

$$m^2 + \frac{K_p m^2\tau^2}{2} - K_p m\tau + K_p = 0 \tag{3.32}$$

The equation above can be solved as a quadratic equation following the algorithm below:

Solving our equation in the form:

$$A x^2 + Bx + c = 0 \tag{3.33}$$

$$\left(1 + \frac{K_p \tau^2}{2}\right) m^2 - K_p m\tau + K_p = 0 \tag{3.34}$$

Using the quadratic formula to obtain a solution for the equation below:

$$m_{1,2} = \frac{K_p \tau \pm \sqrt{K_p^2 \tau^2 - 4\left[1 + \frac{K_p \tau^2}{2}\right]\left[K_p\right]}}{2\left[1 + \frac{K_p \tau^2}{2}\right]} \tag{3.35}$$

The solution to the equation indicates that the discriminant will be less than zero. This implies that the equation has complex roots and so the solution will be as given below:,

$$\theta(t) = e^{\frac{K_p \tau}{2 + K_p \cdot \tau^2}}\left[C_1 \cos\left(\frac{\sqrt{-4K_p - K_p^2 \tau^2}}{2 + K_p \tau^2}\right)(t) + i C_2 \sin\left(\frac{\sqrt{-4K_p - K_p^2 \tau^2}}{2 + K_p \tau^2}\right)(t)\right] \tag{3.36}$$

The solution above shows that with only a naked ‘P’ controller, even with latency taken into account’, will still experience an exponential growth in oscillations should the system encounter a disturbance, and this has been validated experimentally. Based on the above results, a PD-controller was then developed and implemented.

PD- Controller

As has been determined by experiment and observed from the analytical results above, a P-controller alone is not sufficient to stabilize a tilt-wing UAV in roll or pitch. A more robust stabilization system is required. It is here that a PD-controller is developed and implemented in order to provide a quicker response and stabilizes the system in a much smoother manner.

The general equation for a PD controller is as given below:

$$\varphi = -\left[k_p\theta(t) + k_d\dot{\theta}(t)\right] \tag{3.37}$$

$$\varphi(t) = -\left[k_p\theta(t) + k_d\dot{\theta}(t)\right] \tag{3.38}$$

$[k_d]$ is the d coefficient at time. This is the changeable parameter in the model

$\dot{\theta}$ is the angular velocity (rate of change of the pitch angle)

Given that;

$$\varphi = \frac{J_y\ddot{\theta}}{Fh} \tag{3.39}$$

It can be rewritten in the form below,

$$\frac{J_y\ddot{\theta}}{Fh} = -\left[k_p\theta(t) + k_d\dot{\theta}(t)\right] \tag{3.40}$$

$$\ddot{\theta}(t) = \frac{-Fhk_p}{J_y}\theta(t) - \frac{Fhk_d}{J_y}\ddot{\theta}(t) \tag{3.41}$$

Given that;

$$\frac{Fhk_p}{J_y} = K_p \tag{3.42}$$

$$\frac{Fhk_d}{J_y} = K_d \tag{3.43}$$

where K_d is a term for the d-coefficient containing the expression $\frac{Fhk_d}{J_y}$

The second order differential equation describing the dynamics of the system is then written in the form below:

$$\ddot{\theta}(t)+K_d\theta(t)+K_p\theta(t)=0 \tag{3.44}$$

The resulting solution will be a sinusoidal curve whose behavior largely depends on the values of the coefficients k_p and k_d.

The outcome of the second order differential equation would be to determine an optimum relation between K_p and K_d.

As such, the differential equation can be solved in the form,

$$\theta=e^{mt} \tag{3.45}$$

It then becomes;

$$m^2e^{mt}+K_dme^{mt}+K_Pe^{mt}=0 \tag{3.46}$$

The characteristic equation is developed as;

$$m^2+K_dm+K_p=0 \tag{3.47}$$

Solving the discriminant in order to obtain a relation between K_p and K_d, we achieve the following solution;

$$m_{1,2}=\frac{-K_d\pm\sqrt{K_d^2-4K_p}}{2} \tag{3.48}$$

$$K_d^2-4K_p=0 \tag{3.49}$$

$$4K_p=K_d^2 \tag{3.50}$$

It is here that an optimal relationship between K_p and K_d has been achieved.

CHAPTER IV

Methodology

The design of the tilt-wing UAV (Lanner) was made in SOLIDWORKS. Careful consideration was taken regarding the distribution of the components which would be contained within the aircraft. The load distribution of the components is of primary importance as this greatly affects the location of the center of gravity

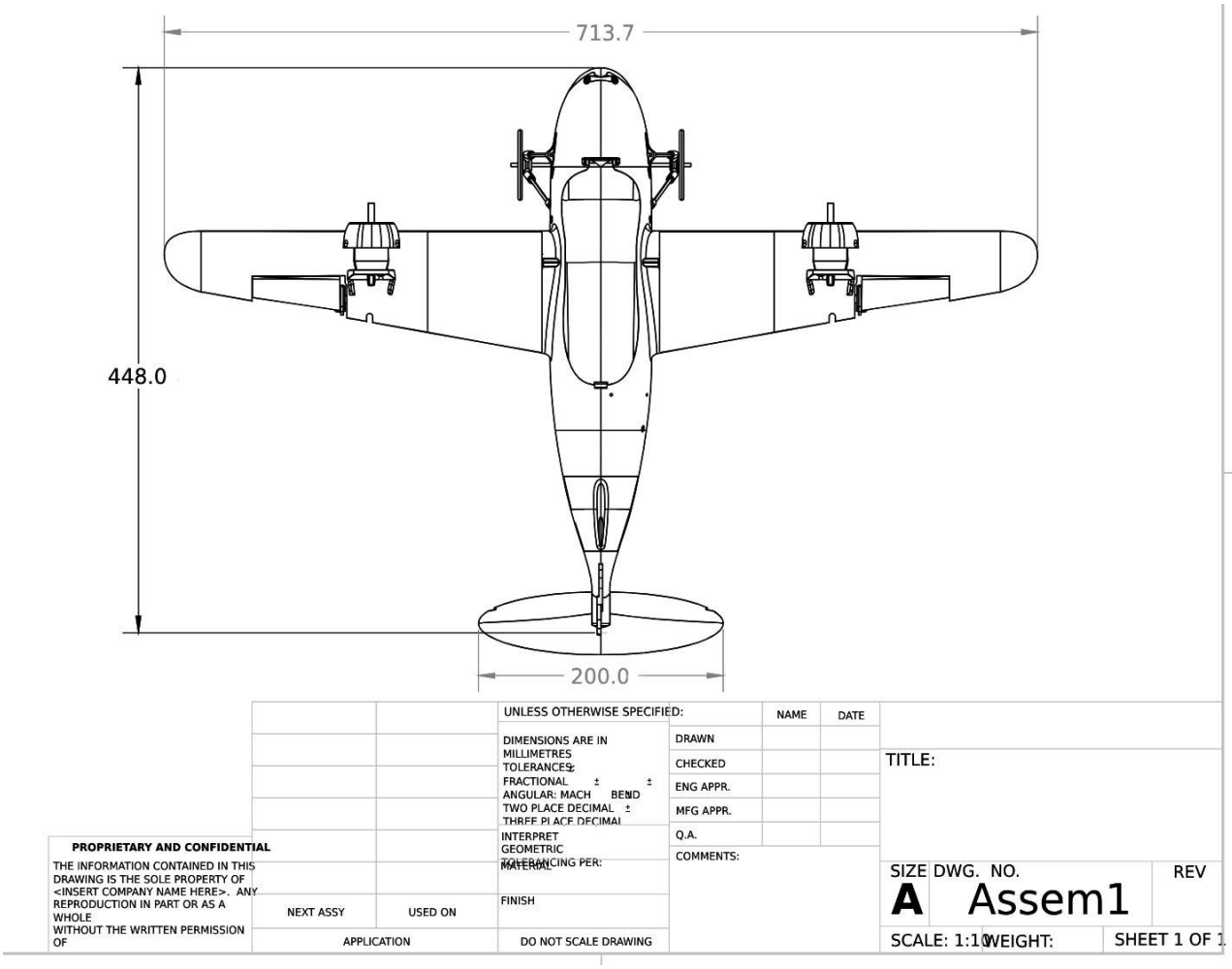

Figure 4.1 Lanner's Top View (Units in mm)

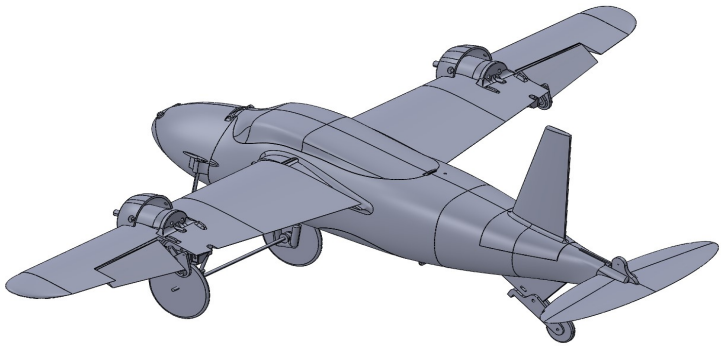

Figure 4.2 Lanner's Isometric View

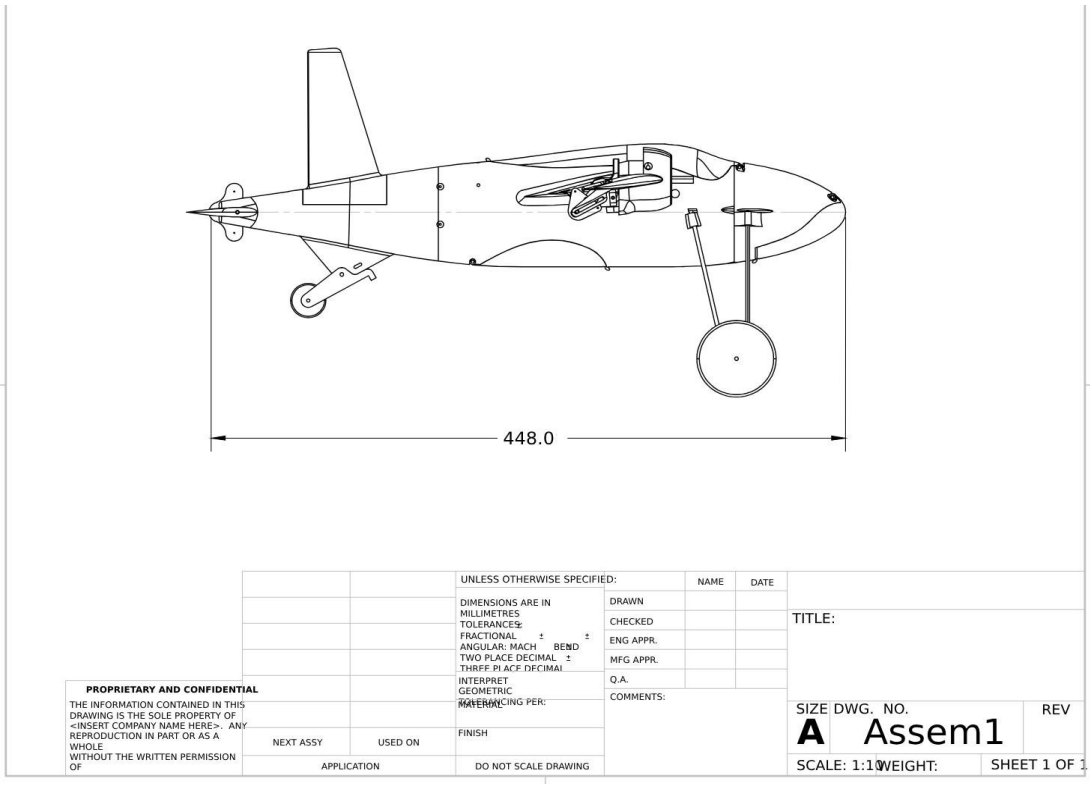

Figure 4.3 Lanner's Side View (Units in mm)

Components On-board The UAV

There are several electrical components which have been used on the tilt-wing UAV. Some of the key components are listed below:

i Servo Motor

A servo motor is a closed-loop servo mechanism that uses position feedback to control its motion and final position (Belal Sebabha et al, 2015) . For its use in this current study, the servo motor is attached to a gear which effectively rotates another gear to which it is attached and in this way, it rotates the wing. The gears have a ratio of 1.8:1.

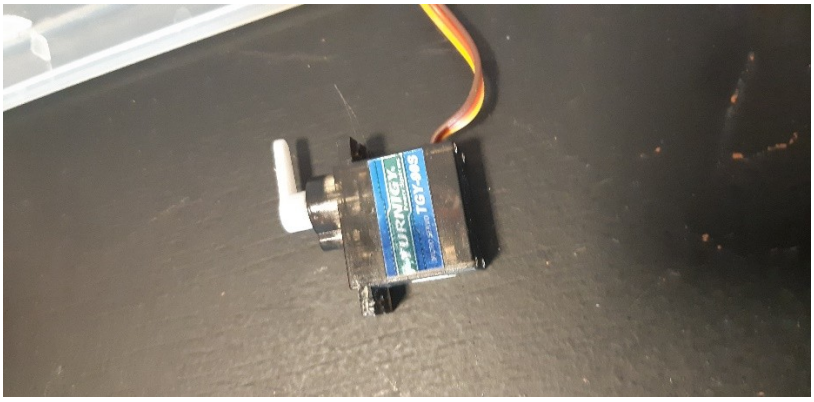

Figure 4.4 Servo Motor

ii Electronic Speed Controller (ESC)

An electronic speed controller is an electronic device which is responsible for controlling the power output and the motors rotational speed in such a way as to meet the operator's requirements (Andrew Gong et al, 2017).

Figure 4.5 An ESC

iii Inertial Management Unit (IMU)

An inertial measurement unit (IMU) is an electrical device which is used to determine the speed, orientation, position and acceleration of an object relative to earth's surface (Aftandil Mammadov et al, 2022). An IMU contains an accelerometer, magnetometer, GPS and gyroscope. The device works by sending information to the flight controller and necessary adjustments and corrections are then made to the tilt-wing actuating mechanism which then stabilizes the UAV in hover mode.

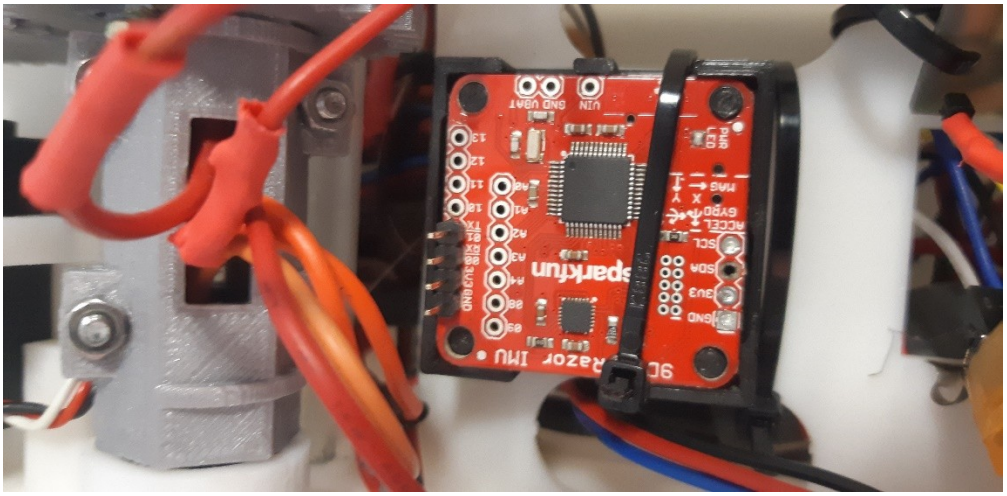

Figure 4.6 An Inertial Measurement Unit (IMU)

In the event that the UAV encounters a disturbance that causes the nose to pitch down, the IMU will detect the negative pitch angle and will, as a result, cause the wing to tilt backwards in such a way as to produce a corrective positive pitching moment and in this way, stabilize the UAV. In the event that the UAV encounters a

disturbance that will cause a positive pitch angle, the IMU will respond in such a way as to produce a corrective negative pitch angle which will cause the UAV to pitch downwards and thus stabilize the UAV in hover flight.

iv Micro-controller

A micro-controller is a compact microcomputer designed to govern system functions. For the current study, the micro-controller utilized is a Teensy board. Teensy, being a USB-based micro-controller, possesses the capability to execute various project types. The micro-controller consists of several essential components, such as an oscillator, AD converter, RAM, microprocessor, program memory, and input/output peripherals.

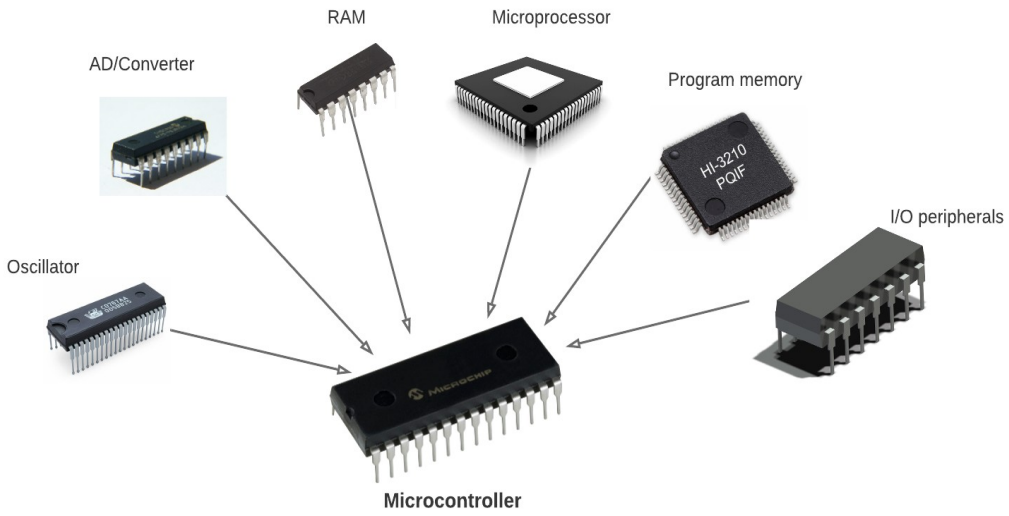

Figure 4.7 Micro-controller

v Voltage Regulator

A voltage regulator is an electrical device which is designed to automatically maintain a constant voltage. The UAV has two voltage regulators. One of 5 volts and the other of 3 volts.

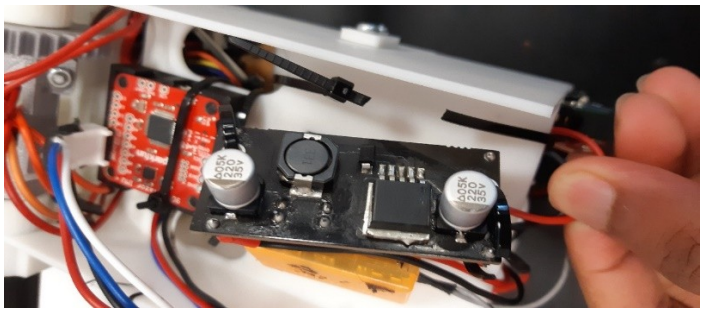

Figure 4.8 3V Voltage Regulator

vi Receiver

Drone receivers are electronic devices responsible for receiving signals from a drone's remote control and converting them into instructions for the drone's flight controller. The flight controller then uses these instructions to make adjustments to the drone's motors, as well as other systems such as tilt-wing and thrust differential, in order to respond to the pilot's commands. Communication between receivers and remote controls generally occurs through radio frequency signals, and receivers are available in various types and frequencies to accommodate different drone designs and usage scenarios. In certain cases, advanced drone receivers may include additional features such as telemetry feedback or support for multiple input channels, enabling more accurate and precise control.

Figure 4.9 Radio Receivers.

The figure shown below shows the layout of the printed circuit board (PCB) that was used in the project under study.

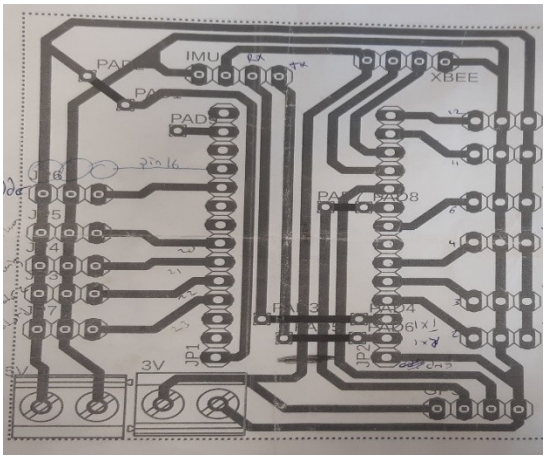

Figure 4.10 PCB Layout

At the beginning of the experiment, the first step is to ensure that the UAV is in neutral equilibrium. Stability can be categorized into two types; static stability and dynamic stability (Lixin Wang et al). Static stability can be further divided into neutral stability, negative static stability and positive static stability. Positive static stability is defined as the tendency of an object to return to a state of equilibrium whereas negative static stability is defined as the tendency for an object to diverge from an initial point of equilibrium after a disturbance.

Neutral equilibrium is defined as the tendency for a body to come to rest at a particular point or orientation after the disturbance is removed.

The entire fuselage of the tilt-wing UAV has been 3D printed using PLA (polyactic acid). PLA was chosen was chosen as it is an easy material to print with, it is typically printed at low temperatures and it has good mechanical properties which satisfy the strength requirements for the current study. Additionally, PLA has an aesthetically pleasing finish.

Design of the Tilt-Wing UAV Test Bench

The fuselage for the UAV under the current study was designed to developed in order to investigate and implement a PID controller to autonomously stabilize the UAV in hover flight

mode. Several versions of the test bench were designed in SOLIDWORKS and 3D printed until a more suitable design was achieved. The ideal design requirements were such that it should be rigid enough to dampen all vibrations coming from the rotations of the motors in order to minimize interference with the PID controller and the actuating gears for the tilt-wing mechanism.

The UAV has been rigorously tested on a test-bench which serves the purpose of minimizing any possible damage to the UAV as whole by limiting any undesirable or unpredictable movements, and in turn, also preventing possible injuries to anyone within the vicinity of the testing area.

The stand and the fuselage are connected by a 3.5mm aluminum rod which passes through both of them. This facilitates the easy rotation of the fuselage.

To prevent the fuselage from toppling over when the motors and propellers are spinning, stoppers are designed and fixed to the stands. These allow the fuselage to have a pitch angle of $\pm 30^{\circ}$.

The figures below show the series of test benches built for the study

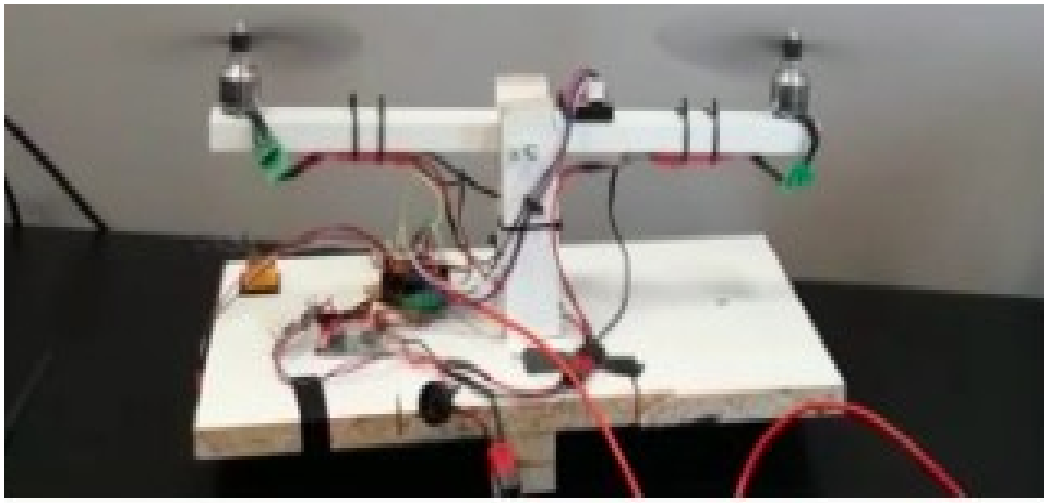

Figure 4.11 Front View for The Test Bench For Roll

Figure 4.12 Pitch Test Bench Version 1.

Fig 4.13 Pitch Test Bench Version 2

Fig 4.14 Roll and Pitch Test Bench

Latency Estimation

One of the greatest contributors to errors encountered during the experiments is latency. Latency can be defined as a delay in the time taken to transmit, receive and implement a given signal to achieve a desired outcome in a system (Mitchell Green et al, 2021). The latency of the system is desired to be as minimal as possible as this will enable the system to respond more quickly to disturbances and thus implement corrective measures which will prevent any potential failures.

For the system under study, the latency has been investigated using only a P-controller as this greatly simplifies the task. It is at this point that several tests were run using different values for the P coefficient.

Selection of The Initial P Coefficient

In order to more accurately estimate an initial value for the P coefficient, a MATLAB script was developed which solves the PID controller equation as a third degree polynomial. Upon obtaining a solution to the polynomial, a graphical user interface was developed which displays the roots of the equation that can be taken as initial estimates. The values can be analyzed

through the GUI by using a slider which when operated, gives a graphical output which shows the growth or decrease in quality of the oscillatory behavior of the system for each corresponding value. It is in this way that the initial value for the P coefficient was estimated.

An initial value of 0.5 was selected for the P-coefficient. Observations were made of the systems response. Both period of oscillations and the amplitude were derived from data streamed from the IMU. Using this data, graphs of amplitude against period were derived. This process was repeated for P coefficient values of 0.4 and 0.6.

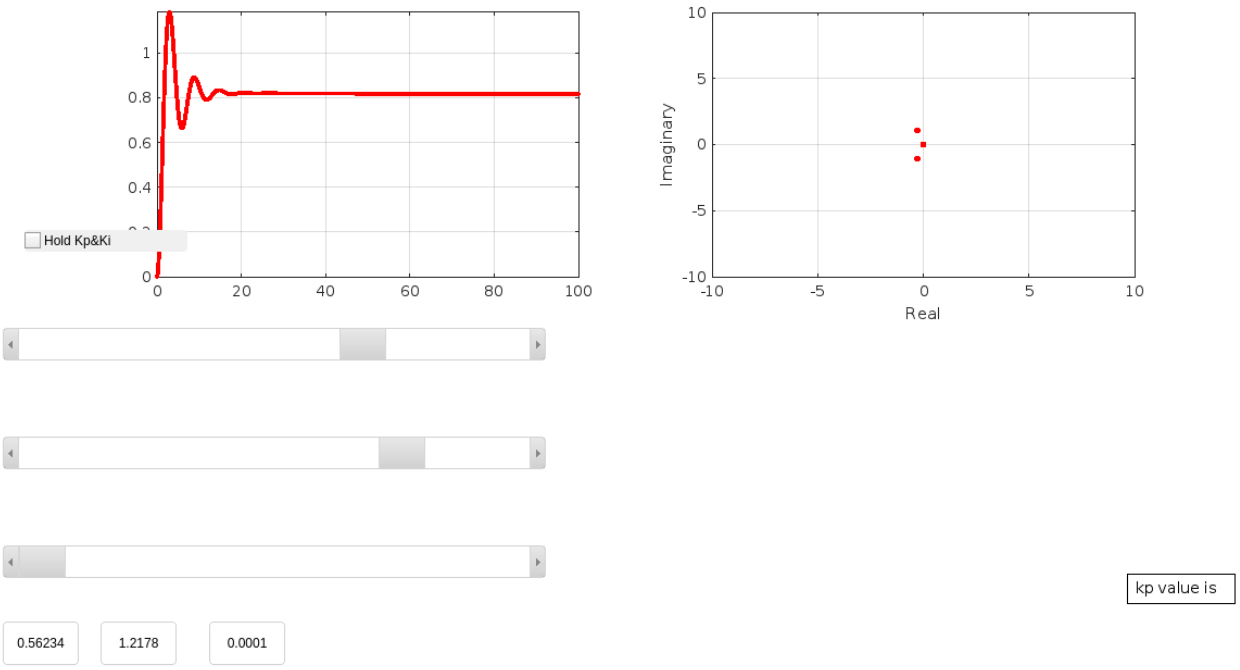

Fig 4.15 MATLAB Graphical user interface aided selection of the initial P-coefficient

CHAPTER V

Results and Discussion

An optimal relationship between the P-coefficient and D-coefficient was sought in order to achieve a solution that stabilizes the UAV when it encounters any disturbances that may effectively change its roll and/or pitch attitude. The achievement of the relationship as expressed in equation (3.50) is what enables the PD-controller to stabilize the UAV. Such a relationship captures the effects that either component has on the other, and this relationship and its ability to stabilize the UAV has been validated experimentally.

Figures 5.1, 5.2, and 5.3 depict a comparison between the anticipated and observed outcomes of the P-controller in pitch control during the experiment. Analyzing the theoretical aspect reveals that a system solely employing a P-controller, along with latency, exhibits sinusoidal oscillations that grow exponentially. This aligns with the experimental findings, although the observations are limited due to the implementation of stoppers in the experiment, preventing the fuselage from overturning, which restricts visibility beyond a certain threshold.

The experimental results fall within a reasonable range, and the disparity between the theoretical and observed values can be reasonably attributed to several factors. Firstly, the presence of friction in the setup, which was not taken into account in the theoretical analysis. Secondly, the servo motors exhibited imperfect performance, contributing to the differences. Lastly, an error was identified in the initial analysis as it failed to consider the moment of inertia from the wings. Therefore, it is crucial to address this oversight in future studies.

In accordance with the theoretical findings, it is observed that the P-controller with a coefficient, kp, set at 0.4 exhibits a slower response to disturbances compared to those with higher kp values.

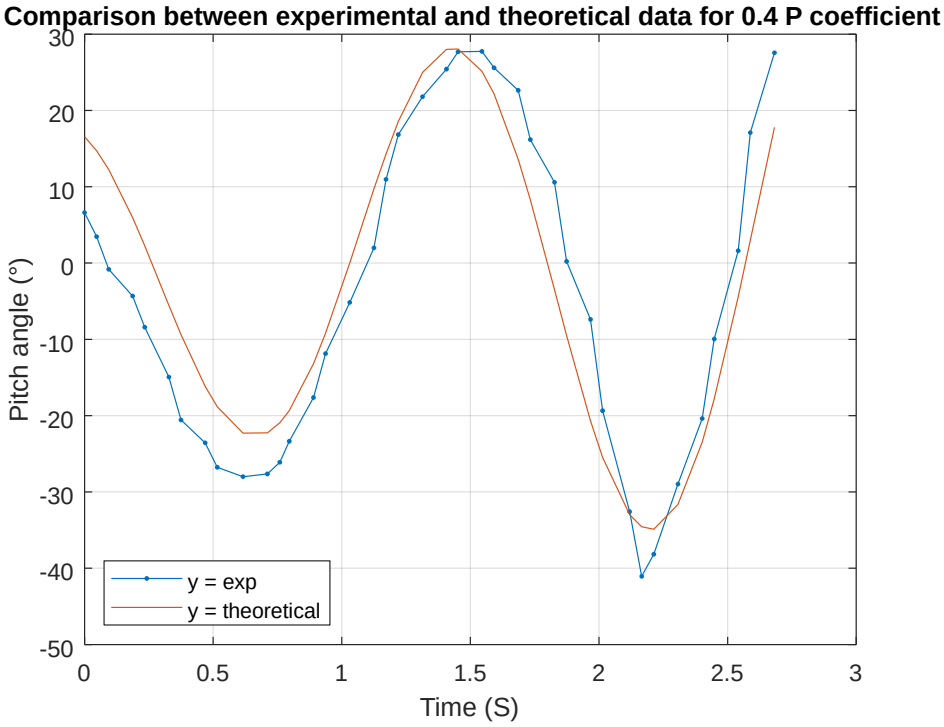

Figure 5.1 Comparison between Experimental and Theoretical Data for k_p value of 0.4

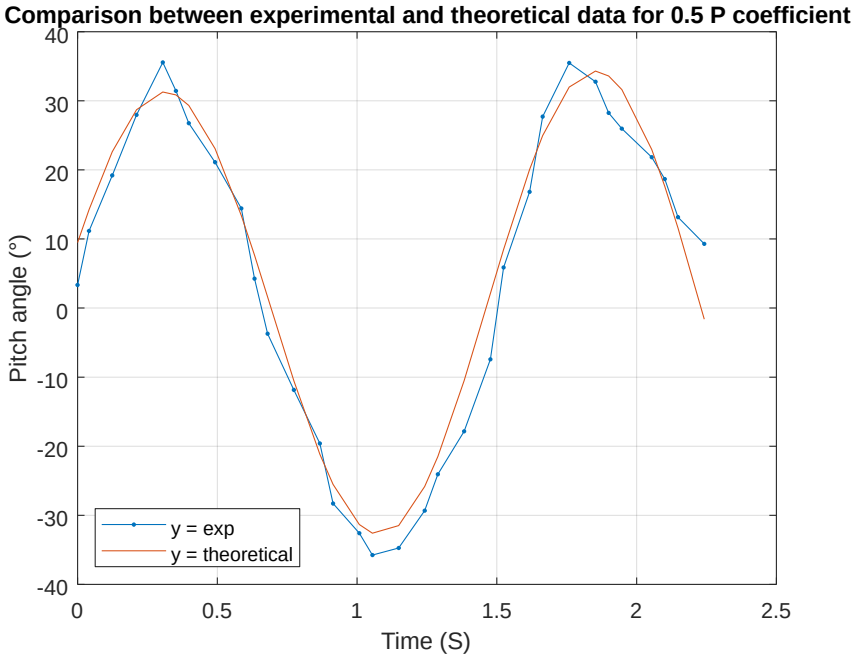

Figure 5.2 Comparison between Experimental and Theoretical Data for k_p value of 0.5

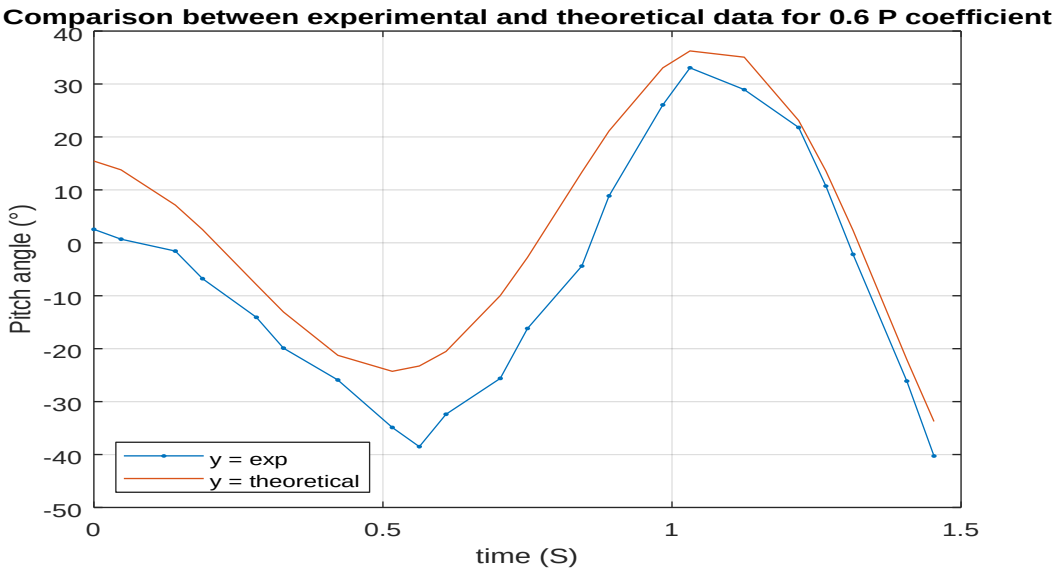

Figure 5.3 Comparison between Experimental and Theoretical Data for k_p value of 0.6

Table 5.1 Comparison of the kp Values

	0.4	0.5	0.6
Standard deviation experimental	20.64567	23.08258	22.34313
Standard deviation theoretical	19.29958	22.2042	21.12483

CHAPTER VI

Conclusion

The UAV under study has been developed with potential applications in heavy payload delivery in mind. With highly optimized hovering capabilities, it will be able to reach and operate in remote areas where conventional transportation systems cannot operate due to the absence of either roads, airports or appropriate landing fields. Sample payloads it would be able to deliver are medical supplies to remote and generally inaccessible areas (hospitals and clinics located in remote areas), equipment required in order to adequately respond to natural disasters and delivery of time-sensitive cargo over long distances.

Previous investigations on the UAV revealed the necessity of a dedicated test-bench for both roll and pitch control, as the aircraft demonstrated satisfactory roll control but relatively poorer performance in pitch control. In this thesis, a test-bench was designed using SOLIDWORKS specifically for assessing roll and pitch control in a tilt-wing UAV, which possesses the capability of vertical takeoff and landing. The primary focus of this study is the examination of roll and pitch control during hover flight. Comparing the theoretical and experimental results demonstrated favorable agreement between the two. P-Controllers with k_p values of 0.4, 0.5, and 0.6 were implemented, and their outcomes were scrutinized to verify the experimental validity and the extent of alignment with the theoretical framework.

Future work to be done on this study will include a refinement of the model and its implementation to the transition to and from forward flight modes.

References

Adnan S. Saeed, Ahmad Bani Younes, Shafiqul Islam, Jorge Dias, Lakmal Senevirante, Gouwei Cai, "A Review on the Platform Design, Dynamic Modeling and Control of Hybrid UAVs", IEEE 2015 International Conference on Unmanned Aircraft Systems (ICUAS)

Aftandil Mammadov, "Analysis of Micro-electromechanical Inertial Measurement Units for Unmanned Aerial vehicle Applications", 2022 Scientific Journal of Silesian University of Technology. Series Transport.

Andrew Gong, Dries Verstraete, "Experimental Testing of Electronic Speed Controllers for UAVs", July 2017 DOI: Conference: 53rd AIAA/SAE/ASEE Joint Propulsion Conference

Belal Sebabha, Hamzeh Alzubhi, Osamah Rawashdeh, "A rotor- Tilt-free tricopter UAV: Design, modelling, and stability control", December 2015 International Journal of Mechatronics and Automation 5(2/3):107-113 DOI:10.1504/IJMA.2015.075956

Guillaume J.J. Ducard, Mike Allenspach b, "Review of designs and flight control techniques of hybrid and convertible VTOL UAVs", Aerospace Science and Technology, Volume 118, November 2021, 107035

H. Yeo, W. Johnson, "Performance and Design Investigation of a Heavy Lift Tilt-Rotor With Aerodynamic Interference Effects", Journal of Aircarft Vol. 46, No. 4, July–August 2009, NASA Ames Research Center, Moffett Field, California 94035 DOI: 10.2514/1.40102

Jeffrey. J Dickeson, David Miles, Oguzhan Cifdaloz, Valana L. Wells, Armando A, "Robust LPV Gain Scheduled Hover-to-Cruise Conversion For a Tilt-Wing Rotorcraft in the Presence of CG Variations", 2007 IEEE American Control Conference

Lixin Wang, Ning Zhang, Hailang Liu, Ting Yue, "Stability Characteristics and Airworthiness Requirements of Blended Wing Body Aircrfat With Podded Engines", Chinese Journal of Aeronautics, June 2022, Volume 35, Issue 6, June 2022, Pages 77-86

Mitchell Green, Danny D. Mann, Ekram Hossain, "Measurement of latency during real-time

wireless video transmission for remote supervision of autonomous agricultural machines”, Computers and Electronics in Agriculture, Volume 190, November 2021, 106475

Appendices

Appendix A.

MATLAB Code for the Comparison between Theory and Experimental Data For 0.5 P-Coefficient.

```
close all
clear

dat = importdata('pitch5trial2.txt');

tvec = dat(:,2)/1000;
angvec = dat(:,1);

%manually put time limits
tmin = 22.5;
tmax = 26.5;

%cut out the zone of interest
zone_inds = (tvec >= tmin) & (tvec <= tmax);
tvec = tvec(zone_inds);
angvec = angvec(zone_inds);

tvec = tvec - tvec(1); %now time will start from 0

figure
plot(tvec, angvec, '.-'); grid on

Fcost_opt = +Inf;

for A = 25:0.1:35

   %DEBUG:
   A

   for freq = 0.8:0.05:1.2
      for phi = 2*pi*(0:0.05:1)
         for  alpha = -0.5:0.02:0.5

            theta_theor = A * (cos((2*pi*freq .* tvec) + phi)) .* (exp(alpha * tvec));
            Fcost = sum((angvec - theta_theor).^2);

            if Fcost < Fcost_opt
```

```
                Fcost_opt = Fcost;
                A_opt = A;
                freq_opt = freq;
                phi_opt = phi;
                alpha_opt = alpha;
            end

        end
    end
  end
end

theta_opt = A_opt * (cos((2*pi*freq_opt .* tvec) + phi_opt)) .* (exp(alpha_opt * tvec));

figure
plot(tvec, angvec, '.-'); grid on; hold on
plot(tvec, theta_opt, '-')
```

Appendix B.

MATLAB Code for the Comparison between Theory and Experimental Data For 0.6 P-Coefficient.

```
close all
 clear

dat = importdata('pitch6trial3.txt');

tvec = dat(:,1)/1000;
angvec = dat(:,5);

% plot(tvec, angvec, '.-'); grid on

%manually put time limits
tmin = 11.6;
tmax = 13.7;

%cut out the zone of interest
zone_inds = (tvec >= tmin) & (tvec <= tmax);
tvec = tvec(zone_inds);
angvec = angvec(zone_inds);

tvec = tvec - tvec(1); %now time will start from 0

figure
plot(tvec, angvec, '.-'); grid on

Fcost_opt = +Inf;

for A = 35:0.1:45

   %DEBUG:
   A

   for freq = 0.8:0.05:1.2
      for phi = 2*pi*(0:0.001:1)
         for  alpha = -0.5:0.02:0.5

            theta_theor = A * (cos((2*pi*freq .* tvec) + phi)) .* (exp(alpha * tvec));
            Fcost = sum((angvec - theta_theor).^2);

            if Fcost < Fcost_opt
```

```
                Fcost_opt = Fcost;
                A_opt = A;
                freq_opt = freq;
                phi_opt = phi;
                alpha_opt = alpha;
            end

        end
    end
  end
end

theta_opt = A_opt * (cos((2*pi*freq_opt .* tvec) + phi_opt)) .* (exp(alpha_opt * tvec));

figure
plot(tvec, angvec, '.-'); grid on; hold on
plot(tvec, theta_opt, '-')
```

Appendix C.

MATLAB Code for the Comparison between Theory and Experimental Data For 0.4-P Coefficient.

```
dat = importdata('pitch4trial1.txt');

tvec = dat(:,1)/1000;
angvec = dat(:,2);

%manually put time limits
tmin =30;
tmax = 31.8;

%cut out the zone of interest
zone_inds = (tvec >= tmin) & (tvec <= tmax);
tvec = tvec(zone_inds);
angvec = angvec(zone_inds);

tvec = tvec - tvec(1); %now time will start from 0

figure
plot(tvec, angvec, '.-'); grid on

Fcost_opt = +Inf;

for A = 20:0.1:28

   %DEBUG:
   A

   for freq = 0.5:0.05:1.0
      for phi = 2*pi*(0:0.01:1)
         for  alpha = -0.5:0.02:0.5

            theta_theor = A * (cos((2*pi*freq .* tvec) + phi)) .* (exp(alpha * tvec));
            Fcost = sum((angvec - theta_theor).^2);

            if Fcost < Fcost_opt
               Fcost_opt = Fcost;
               A_opt = A;
               freq_opt = freq;
               phi_opt = phi;
               alpha_opt = alpha;
```

```
            end

        end
    end
  end
end

theta_opt = A_opt * (cos((2*pi*freq_opt .* tvec) + phi_opt)) .* (exp(alpha_opt * tvec));

figure
plot(tvec, angvec, '.-'); grid on; hold on
plot(tvec, theta_opt, '-')
```

Appendix D.

MATLAB Code for Selecting an Initial Estimate for The P-Coefficient Via a Graphical User Interface

```
close all
clear
global Kd Kp Ki flagKdKpKi
delta_t = 0.001; %time step
T = 100; %simualation time
N = round(T/delta_t);
tvec = (0: N-1) * delta_t;
flagKdKpKi = true;
%add UI components in struct
hs.fig = figure('units','normalized','outerposition',[0 0 1 1]);
% hs.fig = figure('Position',.[0 50 1098 767],'Visible','on', 'Resize','on','Tag','fig');
%hs.btn = uicontrol(hs.fig,'Position',[10 540 200 30],'String','open
pid','Tag','button','Callback','pidscript');
% hs.sP = uicontrol(hs.fig,'Style','slider','String', 'kp','Min',0, 'Max',1, 'Value', 0,...
% 'Position',[10 340 200 30]);
% range = [10^0 10^2];
hs.tD = uicontrol(hs.fig,'style','edit','Position',[10,60,70,40]);%this is the box in which the slider
value is displayed
hs.sD = uicontrol(hs.fig,'style','slider','Position',[10,340,500,30]);
% 'min', log10(range(1)),...
% 'max', log10(range(2)),...
% 'callback', @(src,event)set(src,'UserData',10^get(src,'Value')));
%fun = @(~,e)set(hs.t,'String',num2str(get(e.AffectedObject,'Value')));
hs.tP = uicontrol(hs.fig,'style','edit','Position',[100,60, 70,40]);%this is the box in which the slider
value is displayed
hs.sP = uicontrol(hs.fig,'style','slider','Position',[10,240,500,30]);
%fun = @(~,e)set(hs.t,'String',num2str(get(e.AffectedObject,'Value')));
hs.tI = uicontrol(hs.fig,'style','edit','Position',[200,60,70,40]);%this is the box in which the slider
value is displayed
hs.sI = uicontrol(hs.fig,'style','slider','Position',[10,140,500,30]);
%fun_debug = @(~,e) MyDebugD(get(e.AffectedObject,'Value'), hs.tD,hs.tP)
fun_debug = @(~,e) MyDebugD(get(e.AffectedObject,'Value'), hs.tD, hs.tP, hs.tI);
addlistener(hs.sD, 'Value', 'PostSet',fun_debug);
fun_debug = @(~,e) MyDebugP(get(e.AffectedObject,'Value'), hs.tP);
addlistener(hs.sP, 'Value', 'PostSet',fun_debug);
fun_debug = @(~,e) MyDebugI(get(e.AffectedObject,'Value'), hs.tI);
addlistener(hs.sI, 'Value', 'PostSet',fun_debug);
% hs.tI = uicontrol(hs.fig,'style','edit','Position',[10,60,40,40]);%this is the box in which the slider
value is displayed
```

```
% hs.sI = uicontrol(hs.fig,'style','slider','Position',[10,140,200,30]);
%fun = @(~,e)set(hs.t,'String',num2str(get(e.AffectedObject,'Value')));
% fun_debug = @(~,e) MyDebugI(get(e.AffectedObject,'Value'));
% addlistener(hs.sI, 'Value', 'PostSet',fun_debug);
hs.checkbox = uicontrol(hs.fig,'Style','checkbox','String','Hold Kp&Ki','Value',true,'Position',[30
440 150 20], 'Callback', 'MyCheckBox');
hs.sax = axes(hs.fig,'Position',[.28 .10 .6 .85],'XLim', [-5 5], 'YLim',[-5 5], 'XTick',(-
5:1:5),'YTick',(-5:1:5));
% txtbox = uicontrol(hs.fig,'Style','edit', 'String',"p is",'Position',[30 50 130 20]);
annotation(hs.fig,'textbox', [0.90, 0.1, 0.1, 0.1], 'String', "kp value is " )
while true
theta = ResponseCalc(Kd, Kp, Ki, N, delta_t);
%axes(hs.sax)
subplot(2,2,1)
plot(tvec,theta,'r.-');
grid on;
axis([0, T, -Inf, Inf])
drawnow
f = [1 Kd Kp Ki];
r = roots(f);
subplot(2,2,2)
plot(real(r),imag(r),'r.', 'markersize', 10); grid on;
rmax = max(abs(r));
axlimits = 10.^ceil(log10(rmax));
axis(axlimits*[-1, 1, -1, 1])
ylabel('Imaginary'),xlabel('Real')
drawnow
pause (0.1)
end
```

Appendix E.

C Code for the PID Controller

```
#ifndef VTOL_HOVER_H

#define VTOL_HOVER_H

//ATTENTION: X - front, Y - up, Z - right


float J = 0.0076; //inertia moment along Z-axis

float F0 = 5;

float L = 0.022;

float Lmotor = 0.18; //distance from CG to motor

float Jroll = 0.02; //inertia moment along X-axis



float roll_coef_p = 0.00; //0.15;

float roll_Coef_P = roll_coef_p * F0*Lmotor/Jroll;

float roll_Coef_D = sqrt(3*roll_Coef_P);

float roll_Coef_I = roll_Coef_D*roll_Coef_D*roll_Coef_D / 27;

float roll_coef_d = roll_Coef_D * Jroll/(F0*Lmotor);

float roll_coef_i = roll_Coef_I * Jroll/(F0*Lmotor);;


float roll_coef_p_scaled = roll_coef_p / 57.3;

float roll_coef_d_scaled = roll_coef_d * 50.0/57.3;
```

```
float roll_coef_i_scaled = roll_coef_i / (50.0 * 57.3);



//! coef_p = 0.25 and 0.8 in front of coef_d give good result(pitch)
//float pitch_coef_p = 0.25;
//float pitch_Coef_P = pitch_coef_p * F0*L/J;
//float pitch_Coef_D = 2*sqrt(pitch_Coef_P);
//float pitch_coef_d = 0.8 * pitch_Coef_D * J/(F0*L);
//float pitch_coef_i = 0.0;

    float pitch_coef_p = 0.15; //0.25;  //0.4 - for testbench, and 0.2 - presumably for flight;
    float pitch_Coef_P = pitch_coef_p * F0*L/J;
    float pitch_Coef_D = sqrt(3*pitch_Coef_P);
    float pitch_Coef_I = pow(pitch_Coef_D,3)/27;
    float pitch_coef_d = 0.5 * pitch_Coef_D * J/(F0*L);
    float pitch_coef_i = pitch_Coef_I * J/(F0*L);   //0.4



float pitch_coef_p_scaled = (pitch_coef_p / 57.3) / 1.2;
float pitch_coef_d_scaled = (pitch_coef_d * 50.0/57.3) / 1.2;
float pitch_coef_i_scaled = 0 * pitch_coef_i / (50.0 * 57.3) / 1.2;
```

```
pid_controller<float> pid_hoverpitch(pitch_coef_p_scaled, pitch_coef_i_scaled,
pitch_coef_d_scaled,
                        -90.0, 90.0, -0.99, 0.99, false, 0.0);


pid_controller<float> pid_hoverroll(roll_coef_p_scaled, roll_coef_i_scaled, roll_coef_d_scaled,
                        -90.0, 90.0, -0.99, 0.99, false, 0.0);



class vtol_hover {
  void (vtol_hover::* state)();

  void stby() {
    servo_ch4(rc_ch2() + rc_ch3());
    servo_ch4(rc_ch2() - rc_ch3());

    //servo_ch4(rc_ch2());
    //servo_ch5(rc_ch2());

    //'equalized' motor steering
    //auto handle_throttle = math::map<float>(rc_ch2(), -0.61, 0.84, 1, 0);
    //auto diff_throttle = rc_ch3();
    //auto throttle_left = math::map<float>(handle_throttle*(1 - diff_throttle), 1, 0, -0.4, 0.8);
```

```
  //auto throttle_right = math::map<float>(handle_throttle*(1 + diff_throttle), 1, 0, -0.2, 0.45);


  servo_ch3(rc_ch5());
  servo_ch2(rc_ch4());
//servo_ch2(rc_ch3());


  telemetry_write_ping(imu.roll_raw, imu.pitch_raw, imu.yaw_raw, imu.corr,
                       control_enb(), rc_ch2(), 0, 0, 0, 0);


  if (control_enb())
    state = &vtol_hover::boot;
}


void boot() {
  pid_hoverpitch.reset();
  pid_hoverroll.reset();
  state = &vtol_hover::step;
}


void step() {
  auto pitch_target = math::map_rev<float>(rc_ch5(), -1, 1, -50, 30);
  auto roll_target = math::map_rev<float>(rc_ch3(), -1, 1, -30, 30);
```

```
    //pitch PID
    pid_hoverpitch.set_setpoint(pitch_target);
      auto pitch_signal = pid_hoverpitch.step(imu.pitch_raw);

    //roll PID
    pid_hoverroll.set_setpoint(roll_target);
      auto roll_signal = pid_hoverroll.step(imu.roll_raw);
    //scaling the throttle handle input for motors
    auto handle_throttle = math::map_rev<float>(rc_ch2(), 0.84, -0.61, 0, 1);

    auto throttle_left = math::map_rev<float>(handle_throttle*(1 + roll_signal), 1, 0, -0.19, 0.17);
    auto throttle_right4left = math::map_rev<float>(handle_throttle*(1 - roll_signal), 1, 0, -0.19,
0.17);
    auto throttle_right = 0.00;
    if (throttle_left > 0.15) {
      throttle_right = math::map_rev<float>(throttle_right4left, 0.15, 0.10, 0.385, 0.27);
    }
    else if (throttle_left > 0.05) {
      throttle_right = math::map_rev<float>(throttle_right4left, 0.10, 0.05, 0.27, 0.20);
    }
    else if (throttle_left > 0.00) {
```

```
  throttle_right = math::map_rev<float>(throttle_right4left, 0.05, 0.00, 0.20, 0.08);
 }
 else if (throttle_left > -0.05) {
  throttle_right = math::map_rev<float>(throttle_right4left, 0.00, -0.05, 0.08, 0.00);
 }
 else if (throttle_left > -0.10) {
  throttle_right = math::map_rev<float>(throttle_right4left, -0.05, -0.10, 0.00, -0.13);
 }
 else if (throttle_left > -0.15) {
  throttle_right = math::map_rev<float>(throttle_right4left, -0.10, -0.15, -0.13, -0.20);
 }
 else {
  throttle_right = math::map_rev<float>(throttle_right4left, -0.15, -0.19, -0.20, -0.30);
 }

 //throttle_left = -0.06;
 //throttle_right = 0.08;


//auto throttle_right = math::map<float>(handle_throttle*(1 + roll_signal), 1, 0, -0.2, 0.45);
//auto throttle_left = math::map<float>(handle_throttle*(1 - roll_signal), 1, 0, -0.4, 0.8);
```

```
//pid_test.set_setpoint();

//auto roll_signal = pid_test.step(imu.roll_raw);


//servo_ch3(rc_ch5()); //UAV ailerons


servo_ch3(0.28  + pitch_signal); //tiltwing (we had 0.65 as neutral point)

//servo_ch3(-0.35);


    servo_ch4(0.3); //channel for both motors when working on testbench 2



//servo_ch4(throttle_left); //left motor

//servo_ch5(throttle_right); //right motor



// TELEMETRY_STREAM.print((0.22 + roll_signal));

// TELEMETRY_STREAM.print(" ");

// TELEMETRY_STREAM.print((0.12 - roll_signal));

// TELEMETRY_STREAM.println("");


telemetry_write_ping(imu.roll_raw, imu.pitch_raw, imu.yaw_raw, imu.corr,

                control_enb(), rc_ch2() , rc_ch3(), rc_ch4(), rc_ch5(),control_enb());
```

```
  //telemetry_write_pid_state(pid_roll, pid_pitch);


    if (!control_enb())

      state = &vtol_hover::stby;

  }


  void shutdown() { }


public:

  vtol_hover() : state(&vtol_hover::stby) {}


  void operator()() {(this->*state)();}

}hover;


#endif
```

Appendix X. Turnitin Report

M sc

ORIGINALITY REPORT

12%	9%	5%	5%
SIMILARITY INDEX	INTERNET SOURCES	PUBLICATIONS	STUDENT PAPERS

PRIMARY SOURCES

1	docs.neu.edu.tr Internet Source	2%
2	www.research-collection.ethz.ch Internet Source	1%
3	www.researchgate.net Internet Source	<1%
4	Submitted to Çankırı Karatekin University Student Paper	<1%
5	Submitted to Institute of Technology, Sligo Student Paper	<1%
6	Adnan S. Saeed, Ahmad Bani Younes, Shafiqul Islam, Jorge Dias, Lakmal Seneviratne, Guowei Cai. "A review on the platform design, dynamic modeling and control of hybrid UAVs", 2015 International Conference on Unmanned Aircraft Systems (ICUAS), 2015 Publication	<1%
7	Katzourakis, D I, I Papaefstathiou, and M G Lagoudakis. "An Open-Source Scaled Automobile Platform for Fault-Tolerant	<1%

	Electronic Stability Control", IEEE Transactions on Instrumentation and Measurement, 2010. Publication	
8	"The Proceedings of the 2018 Asia-Pacific International Symposium on Aerospace Technology (APISAT 2018)", Springer Science and Business Media LLC, 2019 Publication	<1 %
9	researchr.org Internet Source	<1 %
10	Submitted to Polytechnic of Turin Student Paper	<1 %
11	shi.buaa.edu.cn Internet Source	<1 %
12	Submitted to Emirates Aviation College, Aerospace & Academic Studies Student Paper	<1 %
13	doaj.org Internet Source	<1 %
14	hdl.handle.net Internet Source	<1 %
15	Vuruskan, Aslihan, Burak Yuksek, Ugur Ozdemir, Adil Yukselen, and Gokhan Inalhan. "Dynamic modeling of a fixed-wing VTOL UAV", 2014 International Conference on Unmanned Aircraft Systems (ICUAS), 2014. Publication	<1 %

16	home.cc.umanitoba.ca Internet Source	<1 %
17	Submitted to University of Alabama Student Paper	<1 %
18	ore.exeter.ac.uk Internet Source	<1 %
19	www.cds.caltech.edu Internet Source	<1 %
20	Guillaume J.J. Ducard, Mike Allenspach. "Review of designs and flight control techniques of hybrid and convertible VTOL UAVs", Aerospace Science and Technology, 2021 Publication	<1 %
21	Submitted to Ibri College of Technology Student Paper	<1 %
22	mobt3ath.com Internet Source	<1 %
23	realpars.com Internet Source	<1 %
24	Submitted to University of Bath Student Paper	<1 %
25	eprints.qut.edu.au Internet Source	<1 %

26	epublications.marquette.edu Internet Source	<1 %
27	Submitted to Imperial College of Science, Technology and Medicine Student Paper	<1 %
28	Submitted to University of Liverpool Student Paper	<1 %
29	Yildiray Yildiz, Mustafa Unel, Ahmet Eren Demirel. "Nonlinear hierarchical control of a quad tilt-wing UAV: An adaptive control approach", International Journal of Adaptive Control and Signal Processing, 2017 Publication	<1 %
30	mafiadoc.com Internet Source	<1 %
31	Submitted to Lincoln Park High School Student Paper	<1 %
32	en.wikipedia.org Internet Source	<1 %
33	openaccess.altinbas.edu.tr Internet Source	<1 %
34	researchrepository.wvu.edu Internet Source	<1 %
35	Submitted to University of Durham Student Paper	<1 %

36	Adam Ragheb, Michael S. Selig. "Improved Methodology for Predicting the Force on Stalled Spinning Wings", 53rd AIAA Aerospace Sciences Meeting, 2015 Publication	<1 %
37	Submitted to Coventry University Student Paper	<1 %
38	open.metu.edu.tr Internet Source	<1 %
39	orca.cardiff.ac.uk Internet Source	<1 %
40	physics.stackexchange.com Internet Source	<1 %
41	www.chegg.com Internet Source	<1 %
42	Navya Thirumaleshwar Hegde, V.I. George, C. Gurudas Nayak, Kamlesh Kumar. "Design, dynamic modelling and control of tilt-rotor UAVs: a review", International Journal of Intelligent Unmanned Systems, 2019 Publication	<1 %
43	www.dtic.mil Internet Source	<1 %
44	Submitted to Fareham College Student Paper	<1 %

45	Submitted to University of Pretoria Student Paper	<1 %
46	Submitted to University of Strathclyde Student Paper	<1 %
47	researchspace.ukzn.ac.za Internet Source	<1 %
48	Pian, . "Incompatible Elements for the Theory of Elasticity", Modern Mechanics and Mathematics, 2005. Publication	<1 %
49	ethesis.nitrkl.ac.in Internet Source	<1 %
50	archive.org Internet Source	<1 %
51	centaur.reading.ac.uk Internet Source	<1 %
52	www.math.chalmers.se Internet Source	<1 %
53	"Proceedings of the Fifth Euro-China Conference on Intelligent Data Analysis and Applications", Springer Science and Business Media LLC, 2019 Publication	<1 %
54	Adnan S. Saeed, Ahmad Bani Younes, Chenxiao Cai, Guowei Cai. "A survey of hybrid	<1 %

	Unmanned Aerial Vehicles", Progress in Aerospace Sciences, 2018 Publication	
55	L. Roca, E. Oset. "On the hidden charm pentaquarks in $$\Lambda _b \rightarrow J/\psi K^- p$$ Λ b → J / ψ K - p decay", The European Physical Journal C, 2016 Publication	<1 %
56	Suiyuan Shen, Jinfa Xu, Qingyuan Xia. "A Fuzzy Backstepping Attitude Control Based on an Extended State Observer for a Tilt-Rotor UAV", Aerospace, 2022 Publication	<1 %
57	vdocument.in Internet Source	<1 %
58	www.coursehero.com Internet Source	<1 %
59	www.xponential.org Internet Source	<1 %
60	Philipp Hartmann, Carsten Meyer, Dieter Moormann. "Unified Velocity Control and Flight State Transition of Unmanned Tilt-Wing Aircraft", Journal of Guidance, Control, and Dynamics, 2017 Publication	<1 %
61	apps.dtic.mil Internet Source	<1 %

62	etd.aau.edu.et Internet Source	<1 %
63	fenix.tecnico.ulisboa.pt Internet Source	<1 %
64	wlv.openrepository.com Internet Source	<1 %
65	www.anurac.de Internet Source	<1 %
66	www.diagnostyka.net.pl Internet Source	<1 %
67	www.ideals.illinois.edu Internet Source	<1 %
68	www.scilit.net Internet Source	<1 %
69	www.ugent.be Internet Source	<1 %
70	Jay Gundlach. "Designing Unmanned Aircraft Systems", American Institute of Aeronautics and Astronautics (AIAA), 2012 Publication	<1 %

Exclude quotes	Off	Exclude matches	Off
Exclude bibliography	Off		